THE ASTROPHYSICAL JOURNAL, 262:529–553, 1982 November 15

AN OPTICAL AND RADIO INVESTIGATION OF THE RADIO GALAXY 3C 305

T. M. HECKMAN[1,2,3]
Astronomy Program, University of Maryland; and Steward Observatory
G. K. MILEY[1,2]
Sterrewacht Leiden, The Netherlands; and Kitt Peak National Observatory[4]
B. BALICK[1,2]
Department of Astronomy, University of Washington
AND
W. J. M. VAN BREUGEL[2,3] AND H. R. BUTCHER[2]
Kitt Peak National Observatory[4]
Received 1981 December 4; accepted 1982 May 18

ABSTRACT

We report the results of a detailed investigation of the unusual radio galaxy 3C 305. The associated radio source is much smaller (~ 3 kpc) than typical double radio sources but is comparable to them in luminosity ($L_R \approx 10^{42}$ ergs s^{-1}). It is identified with a galaxy having some of the characteristics of a spiral and a bright, extended emission-line region. We have carried out an intensive multiwavelength study of 3C 305 using radio and optical imaging as well as slit spectroscopy.

The most important results are several relationships which appear to exist between the (z-shaped) optical emission-line region and the radio source. First, the morphologies and size scales of the radio and line-emitting regions are very similar. Second, the radio polarization is strongly anticorrelated with the presence of the emission-line gas, the latter having a column density adequate for Faraday depolarization of the radio continuum. Third, the emission-line profiles are very broad (500–800 km s^{-1}) and blue-asymmetric near the strong radio emission but not elsewhere. Fourth, the emission-line gas appears to be in approximate pressure balance with the radio-emitting plasma and to have a kinetic energy similar to the (minimum) energy in the synchrotron radio source.

The lack of detectable nonstellar nuclear optical continuum and the absence of a radial decline in ionization state are inconsistent with photoionization of the emission-line gas by a central nonthermal source. We argue that the emission-line region is instead likely to be powered by the radio jets. Kinetic energy in the jets may be transferred to the interstellar medium, thereby ionizing the ambient gas and possibly driving it away from the radio source. The kinematics of the line-emitting gas close to the radio source are consistent with this outflow model, but the large-scale velocity gradients also suggest that the gas is rotating around the galaxy minor axis. A diffuse ambient medium in pressure equilibrium with the emission-line clouds could confine the radio lobes by static thermal pressure, or by ram pressure if the *lobes* are advancing with velocities of a few hundred kilometers per second. However, the radio source/emission-line energetics indicate that energy is being supplied by the *jets* at velocities much greater than 10^3 km s^{-1}.

We suggest that the unusual nature of the radio source and that of the parent galaxy are connected. The dust, ionized gas, young stars, and faint one-armed spiral may be the result of a recent merger of a luminous early-type galaxy and a late-type galaxy. This merger may have triggered the ejection of radio plasma into the relatively dense interstellar medium supplied by the late-type galaxy.

Subject headings: galaxies: individual — galaxies: internal motions — galaxies: structure — radio sources: galaxies

I. INTRODUCTION

One of the most fascinating questions in extragalactic astronomy concerns why strong extended radio emission is associated with active elliptical galaxies but not with active spiral galaxies. A radio galaxy which may be relevant to this problem is 3C 305.

[1]Visiting Astronomer, Kitt Peak National Observatory.
[2]Visiting Astronomer, National Radio Astronomy Observatory, which is operated by the Associated Universities, Inc., under contract with the National Science Foundation.
[3]Work begun while at Sterrewacht Leiden.
[4]Operated by the Association of Universities for Research in Astronomy, Inc., under contract with the National Science Foundation.

This radio galaxy, for which we list some parameters in Table 1, has several unusual properties. First, the *size of the radio source* is an order of magnitude smaller than that typically seen for such powerful, steep spectrum sources (cf. Miley 1980). Second, the galaxy with which 3C 305 is associated is quite peculiar and has some of the characteristics of a *spiral galaxy*. Indeed, the faint one-armed spiral feature, the thin dust absorption lane crossing the nucleus, and the "general veil of obscuration" across the galaxy led Sandage (1966) to classify it as an Sa(pec). Third, a bright region of spatially *extended emission lines* surrounds the optical nucleus of the galaxy (Sandage 1966).

Because it has this combination of unusual properties, we decided to conduct a detailed radio and optical study of 3C 305. The most important result of the investigation is the demonstration of a striking relationship between the line-emitting gas and the radio source.

The observations and their calibration and reduction are described in § II. The results are presented in § III and discussed in § IV. We consider the evidence for the relation between the radio source and the emission-line gas. We then explore the kinematics and ionization of the gas, and also discuss how the gas can play a role both in forming the morphology of the radio source and in producing the radio emission. Finally, the relevance of our conclusions regarding the nature of 3C 305 for the more general study of active galaxies is given in § V.

This paper is unusually long, containing a large number of detailed data which provide a unique vantage point from which the physics of an extragalactic radio source can be studied. For the reader who wishes to extract from this only the primary conclusions and something of the flavor of our investigation, we advise skimming through § III, and carefully reading the Abstract, §§ IV*a*, IV*e*, and V. We hope the critical reader with more curiosity (and perseverance) will be rewarded by a more thorough consideration of the paper.

TABLE 1

GLOBAL PROPERTIES OF 3C 305[a]

Radio:	
Flux density (178 MHz)	15.6 Jy
Monochromatic power (178 MHz)	5×10^{25} W Hz^{-1}
Spectral index	0.86
Maximum observed extent	13″.5 (11 kpc)
Optical:	
Redshift (heliocentric, optical)	0.0417 ± 0.0002
Galaxy Type	Sa pec, S0 pec, or E pec
Absolute Magnitude, M_v	-22.6
Color, $B-V$	0.76
Maximum observed extent of galaxy	45″×35″ (37×29 kpc)
Maximum observed extent of emission lines	16″ (13 kpc)

[a]Here and throughout the paper we assume a value of $H_0 = 75$ km s^{-1} Mpc^{-1} for the Hubble constant.

II. OBSERVATIONS AND REDUCTION

A summary of the various observations that we made on 3C 305 is presented in Table 2, and some morphological parameters derived from our data are listed in Table 3.

a) *Radio Imaging*

The radio observations were conducted at frequencies of 4885 MHz (6 cm) and 15 GHz (2 cm) using the Very Large Array (VLA) (Thompson *et al.* 1980). The configuration of the partially completed VLA at the time of the 6 cm observations is given in Table 4. The 2 cm observations were undertaken with the complete VLA in the standard B configuration (Thompson *et al.* 1980).

The source 3C 305 was observed for a 12 hour period at 6 cm. The phases and amplitudes of both the crossed and parallel hand correlators were calibrated with respect to 3C 286, measurements of which were interspersed with those of 3C 305 about every 30 minutes. The data were of excellent quality.

The calibrated visibility data were transformed to maps using the VLA fast Fourier transform algorithm. Using different tapering functions, maps of various resolutions were produced. These "dirty" I, Q, and U maps were cleaned and restored (Högbom 1974; Schwarz 1978) using independent software at the VLA and at Leiden. There was no significant difference between the Leiden and VLA cleaned maps. Since the tapered, low-resolution maps showed no evidence for structure not seen in the untapered maps, only the latter (restoring beam 0″.5 circular Gaussian) were used for further analysis.

The 2 cm observations spanned a period of 8 hours. Calibration and reduction proceeded as in the case of the 6 cm observations, except that the observations of the calibrator (3C 287) were taken every ~15 minutes. The maps were cleaned only at the VLA, in this case, and restored with a 0″.36 circular Gaussian for the untapered data.

b) *Optical Imaging*

The optical imaging was conducted using the ISIT vidicon Video Camera at Kitt Peak National Observatory (Robinson *et al.* 1979).

Several 13 minute integrations on 3C 305 were made. First, using the 4 m telescope, a broad-band image was taken through a standard V filter. Second, an exposure was made through a narrow-band interference filter whose wavelength response was centered on the redshifted Hα and [N II] $\lambda\lambda$6548, 6584 emission lines. A corresponding "off-band" image was obtained through a similar narrow-band interference filter centered on the continuum ~100 Å shortward of the redshifted Hα and [N II]. An analogous set of on- and off-band images were obtained for the [O III] λ5007 line using the 2.1 m telescope.

TABLE 2

VARIOUS OBSERVATIONS USED IN THIS INVESTIGATION

Type of Observation	Radio Imaging	Optical Imaging			Optical Spectroscopy	
		Broad Band	Narrow Band		4" Aperture	2" Slit
Observatory	NRAO	KPNO	KPNO	KPNO	KPNO	KPNO
Telescope	VLA	4 m	4 m	2.1 m	2.1 m	4 m
Ancillary Instrument	...	ISIT Video Camera	ISIT Video Camera	ISIT Video Camera	IIDS	HGVS
Wavelengths	λ6 cm, λ2 cm	(V)	6584 Å	5223 Å	4550 Å (a) 6250 Å (b)	See Table 5
Bandwidth or Wavelength Resolution	50 MHz	(V)	74 Å	55 Å	6.5 Å	See Table 5
Spatial Resolution or Seeing	0".5, 0".36	1".0–1".5	1".0–1".5	2"	...	2" slit
Field Size or Wavelength Range	102", 77"	70" × 70"	70" × 70"	130" × 130"	1800 Å	166" (See Table 5)
Pixel Size	0".2, 0".15	0".29 × 0".29	0".29 × 0".29	0".55 × 0".55	...	1".3
Number of Pixels	512 × 512	256 × 256	256 × 256	256 × 256	1048	128 × 512
Dates	1980 Feb., 1981 May	1980 Mar.	1980 Mar.	1981 Jan.	1980 Dec.	1980 May
Purpose of Observations	Morphology of radio intensity & polarization	Morphology of galaxy	Morphology of Hα + [N II]	Morphology of [O III]	Line intensities	Morphology of relative line ratios + kinematics

TABLE 3

EXTENT AND ORIENTATION OF THE OBSERVED COMPONENTS OF 3C 305[a]

Radio Source	Line Emission	Galaxy
Nucleus: 0".6×(<0.3") in PA (64°)		Dust Lane: Extended in PA (120°) Passes within (2") to SW of nucleus
Nucleus to E. Lobe Peak: 2".1±0".1 in PA 42°±1°	Nucleus to E. Lobe Peak: 2".5±0".3 in PA 56°±4°	
Size of E. Lobe: 0".5(transverse)×0".65		
Nucleus to W. Lobe Peak: 1".6±0".1 in PA -137°±1°	Nucleus to W. Lobe Peak: 2".3±0".5 in PA -130°±5°	"Spiral Arm": Wraps from (25") in PA (160°) counterclockwise through one turn into nucleus
Size of W. Lobe: 0".4		
Nucleus to Inner Knots in Jets: (0".9) in PA (54°/-126°)		
Jet Width: <0".3		
East Arm: (8".5) in PA 139°±3°	East Arm: (8") in PA 111°±5°	
West Arm: (7") in PA 137°(curving)	West Arm: (6") in (PA 122°)	
Total Extent: (13".5) in PA (115°)	Total Extent: (16") in PA (95°)×(3") wide	Total Extent: (40"×25") in PA 75°±5°

[a]Quantities in parentheses are highly uncertain. Note that for H_0 = 75 km s^{-1} Mpc^{-1}, 1" = 800 pc.

For all the various images, spatial irregularities in the response of the Video Camera were removed using standard flat-field calibration observations, and the spatial distortion in the image was removed in the usual way (see Butcher, van Breugel, and Miley 1980 for details). The narrow-band images were scaled to correct for known differences in the filter throughputs, and brought into correct registration (aligned) using parameters determined from observations of stars. The off-band image was then digitally subtracted from the on-band image to remove the stellar continuum. No attempt was made to calibrate the imaging data in units of absolute flux.

c) *Optical Spectroscopy*

Information on spatial variations in the emission-line gas was obtained from long-slit spectra taken with the High Gain Video Spectrometer (HGVS) in conjunction with the Ritchey-Chrétien spectrograph on the KPNO 4 m telescope. The HGVS consists of an SIT vidicon coupled to a three-stage image tube. Further details concerning the HGVS observations are given in Tables 2 and 5. The latter table summarizes the variety of slit position angles and gratings used.

In a manner similar to the Video Camera images, the HGVS spectra were calibrated for variations in pixel-to-pixel sensitivity and nonuniform slit illumination. He-Ne-Ar comparison spectra were obtained adjacent in time to each 3C 305 observation in order to correct for time variable changes in the image distortion and zero-point wavelength. The absolute wavelengths are uncertain by $\sim$0.75 channels ($\sim$30 km s^{-1} in the highest resolution data), while wavelength changes along the slit can be measured to a precision of $\sim$0.25 channels in high signal-to-noise data. No evidence for significant "beam pulling" caused by accumulation of charge on the SIT (Schechter and Gunn 1979) was found in our data.

No attempt was made to measure absolute line intensities or even absolute line ratios. However, *changes* in line ratios along the slit (relative ratios) are measurable with a precision of $\sim$5–10% for strong lines and 15–25% for weak lines.

The two-dimensional spectra were analyzed row-by-row by fitting sets of Gaussian profiles to the emission lines. Multiple Gaussian components representing kinematically distinct components in the line profile were fitted simultaneously when warranted. Overlapping lines of different species were de-blended in an analogous manner. From the parameters of these fits, the flux, center velocity, and width (FWHM) of each emission line were obtained. The velocities along the slit at a given position angle for the different atomic species were found to agree to within the estimated errors, as

TABLE 4

VLA CONFIGURATION DURING 6 CENTIMETER OBSERVATIONS

Antenna Number	Station	Distance from Array Center (km)
2.....	W32	5.22
3.....	E1	0.038
4.....	W16	1.59
5.....	E2	0.044
6.....	W24	3.19
7.....	E4	0.15
9.....	W48	10.47
10.....	E3	0.09
12.....	E48	10.47
13.....	E12	0.97
14.....	W56	13.64
15.....	W64	17.16
16.....	E18	1.95
17.....	W8	0.48
18.....	E24	3.19
19.....	N32	4.71
20.....	N2	0.055
21.....	N8	0.44
22.....	N6	0.27

were the nuclear velocities of all the lines measured. The flux level of the continuum was also plotted along the slit, and the position of the peak relative to the line emission was found to be in excellent agreement with the Video Camera images.

Red and blue spectra of the bright core of 3C 305 were obtained with a 4″ circular aperture using the Intensified Image Dissector Scanner (IIDS) on the KPNO 2.1 m telescope. Observations of a quartz lamp were used to correct the data for small-scale irregularities in the image-tube response, and observations of several standard stars were used to put the data on a relative flux scale. The red and blue spectra were joined by matching fluxes in the ~100 Å region of overlap. Since the observing conditions were not photometric, no attempt has been made to place the data on an absolute flux scale. Further details concerning the procedure used in the IIDS reduction and analysis can be found in Heckman, Balick, and Crane (1980).

TABLE 5

PARAMETERS OF SLIT SPECTRA[a,b]

No.	λ Coverage (Å)	λ Resolution (Å)	P.A. (°)	Integration Time (min)
1.....	4843–5529	4.4	57	52
2.....	4843–5529	4.4	90	26
3.....	4998–5340	2.2	100	13
4.....	4997–5338	2.2	150	6.5
5.....	4997–5339	2.2	57	13
6.....	6489–7171	4.4	57	52
7.....	6489–7171	4.4	90	26
8.....	3534–4869	8.6	57	26
9.....	3528–4863	8.6	90	26

[a]Slit width 2″ in all cases.
[b]Pixel size 1.″3 in all cases.

III. RESULTS

a) Radio Imaging

i) *Intensity Distribution*

The present 6 cm radio map made with 0.″5 resolution (Fig. 1*a*) is similar in most essential aspects to the map at 75 cm with 0.″8 resolution by Lonsdale and Morison (1980), and shows 3C 305 to consist primarily of a small, bright triple source (ACB) extended about 3.″5 (~3 kpc) in P.A. ~43°. Near A and B (nomenclature of Lonsdale and Morison) are regions of diffuse, low surface brightness radio emission ("arms"), A′ and B′, extended perpendicular to the bright triple. The total size of the radio emission in 3C 305 is then 13.″5 (~11 kpc). The overall "rotational symmetry" of the source noted by Lonsdale and Morison is not pronounced in our map due to the presence of the feature A″ which was not seen on their map. The absence of this feature at 75 cm is not likely to be due to A″ having a relatively flat spectral index, since it is of approximately the same relative strength in maps of 3C 305 made at 2 cm and 20 cm with the VLA (Miley *et al.* 1982). It is more likely that this feature was either entirely resolved by the relatively long baselines of the Jodrell Bank Multi-Telescope Radio-linked Interferometer (MTRLI) or that it may have been missed in the closure phase mapping technique used by Lonsdale and Morison. They noted that 15% of the total flux density of 3C 305 was not accounted for in their 75 cm map, which could easily explain the discrepancy.

The 2 cm intensity map (Fig. 1*b*) shows the core source to be connected to the two lobes (A and B) by narrow, collimated structures ("jets"). Both jets have brightness enhancements (knots) located approximately halfway between the core and each respective lobe. The orientation of the innermost part of the jets is 54° ± 2°, an offset of ~11° from that of the lobes. The bright part of the radio source is "crooked" with small-scale wiggles superposed on an overall open S shape. These features can be even more clearly seen in a map at 18 cm with 0.″25 resolution (Lonsdale *et al.* 1981).

The source 3C 305 appears to have a steep nonthermal radio spectrum between 75 cm and 2 cm. No flat-spectrum nuclear core was detected.

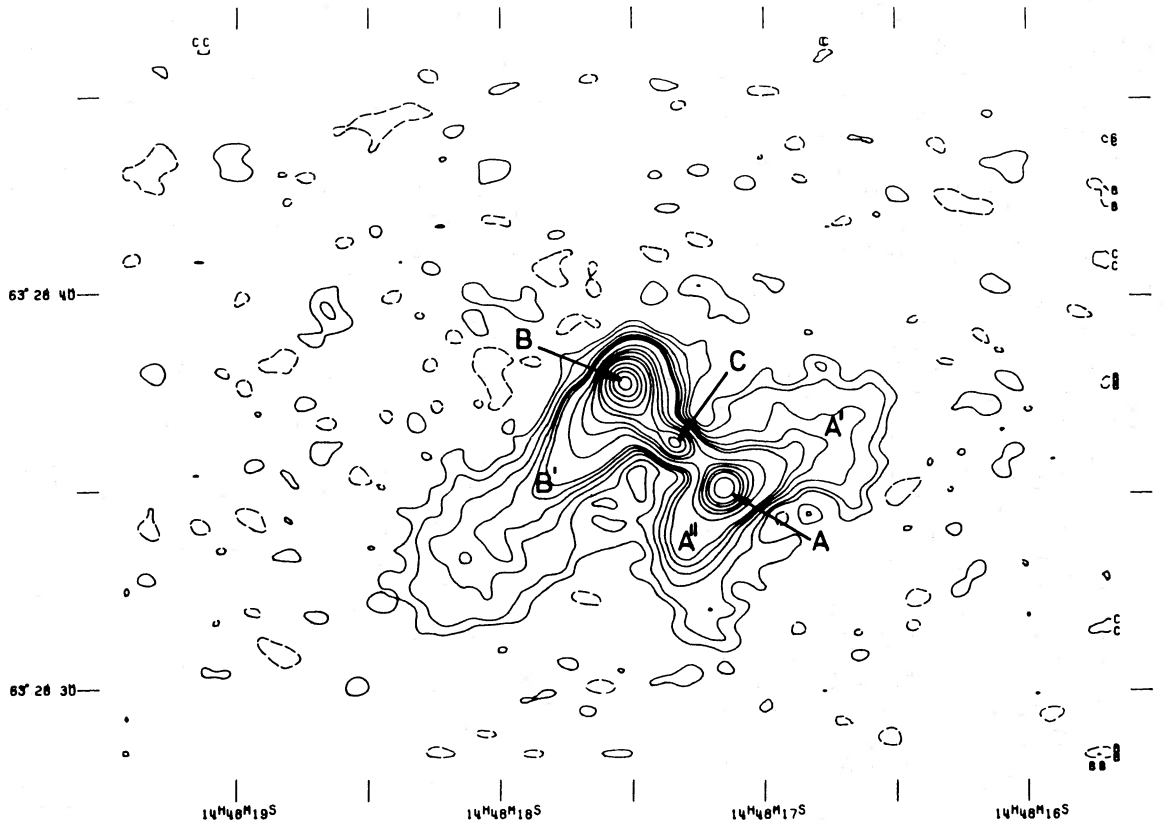

FIG. 1*a*

FIG. 1.—Contour representations of the VLA (*a*) 6 cm and (*b*) 2 cm total intensity maps. The contours for 6 cm are in units of −1.0 (*dashed*), −0.5 (*dashed*), 0.5, 1, 2, 3, 4, 5, 10, 15, 20, 29, 38, 60, 90, 120, 160, 200 mJy per restoring beam (0″.5 FWHM circular Gaussian). The contours for 2 cm are in units of −0.6 (*dashed*), 0.6, 0.78, 1.05, 1.42, 1.87, 2.5, 3.31, 4.52, 6.02, 7.83, 10.54, 14.16, 18.67, and 25.0 mJy per restoring beam (0″.36 FWHM circular Gaussian). The scale in the λ2 cm map is given by the tick marks at 4″ intervals.

TABLE 6

SOME APPROXIMATE MINIMUM-ENERGY PARAMETERS FOR THE RADIO SOURCE

Component	Lobes (A, B)	Nucleus (C)	Arms (A′, A″, B′)	Jet
Internal energy (ergs)	1.0×10^{55}	$\leq 3.0\times10^{54}$	6.0×10^{55}	$\leq 6.0\times10^{54}$
Magnetic field (gauss)	3.0×10^{-4}	$\geq 3.0\times10^{-4}$	3.2×10^{-5}	$\geq 1.0\times10^{-4}$
Internal pressure (dyn cm^{-2})	3.0×10^{-9}	$\geq 3.0\times10^{-9}$	4.1×10^{-11}	$\geq 6.0\times10^{-10}$
Radiative lifetime at 2 cm (yr)	4.0×10^{4}	$\leq 4.0\times10^{4}$	1.0×10^{6}	$\leq 2.0\times10^{5}$
Depolarization ($n_e\phi_p$ in cm^{-3}) ...	$\geq 1.0\times10^{-2}$	$\geq 2.0\times10^{-2}$	...	$\geq 3.0\times10^{-2}$

From both the 2 cm and 6 cm maps, we have derived the parameters listed in Table 6 (minimum internal energy, pressure, magnetic field, etc.). These parameters were calculated making the usual assumptions—namely, a filling factor for the synchrotron emitting plasma equal to unity, equal energies in the electrons and heavy particles, a radio spectrum extending from 10 MHz to 100 GHz, and cylindrical symmetry for the radio components. Since neither the nuclear source nor the jets were resolved in the transverse direction, we have only the appropriate limits to these quantities at these locations.

ii) *Polarization Distribution*

The 5 GHz polarization data are shown in Figures 2 and 3. Most remarkable is the presence of a large region in the source which has extremely low percentage polarization at 5 GHz. This is rarely seen in extended extragalactic radio sources. There are also large gradients in the percentage polarization which range from <1% to

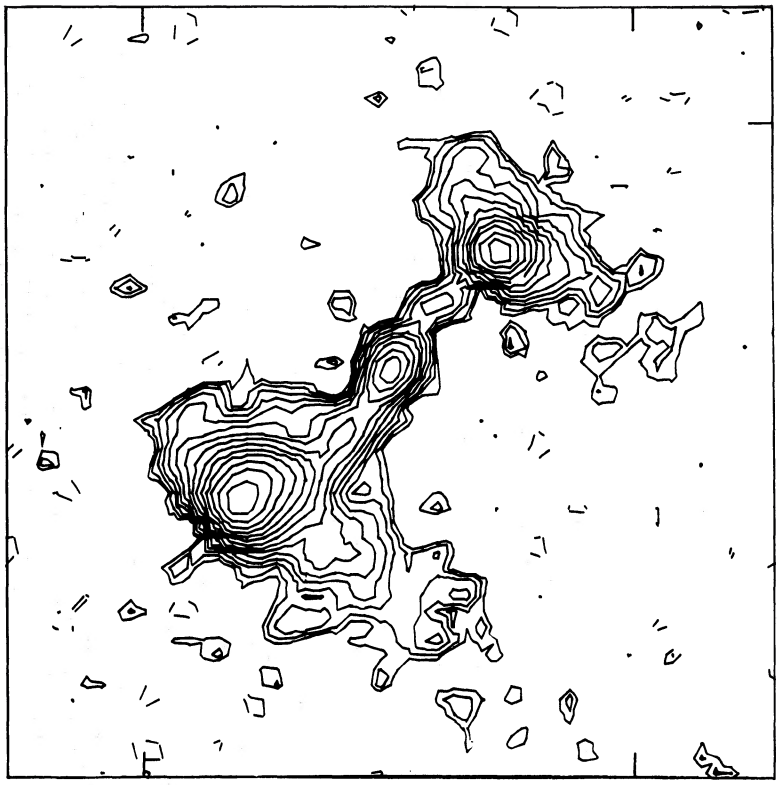

FIG. 1*b*

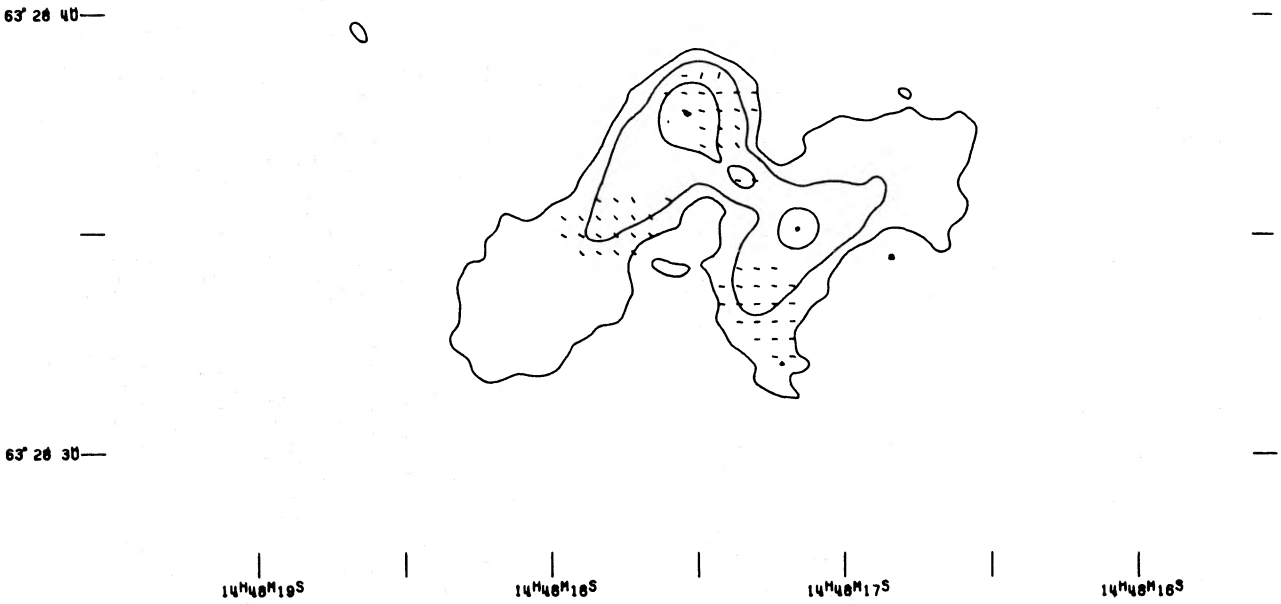

FIG. 2.—Electric field 6 cm polarization vectors superposed on a contour map of the 6 cm total intensity (contour levels at 1, 4, and 30 mJy per restoring beam). The scale and orientation are as in Fig. 1*a*.

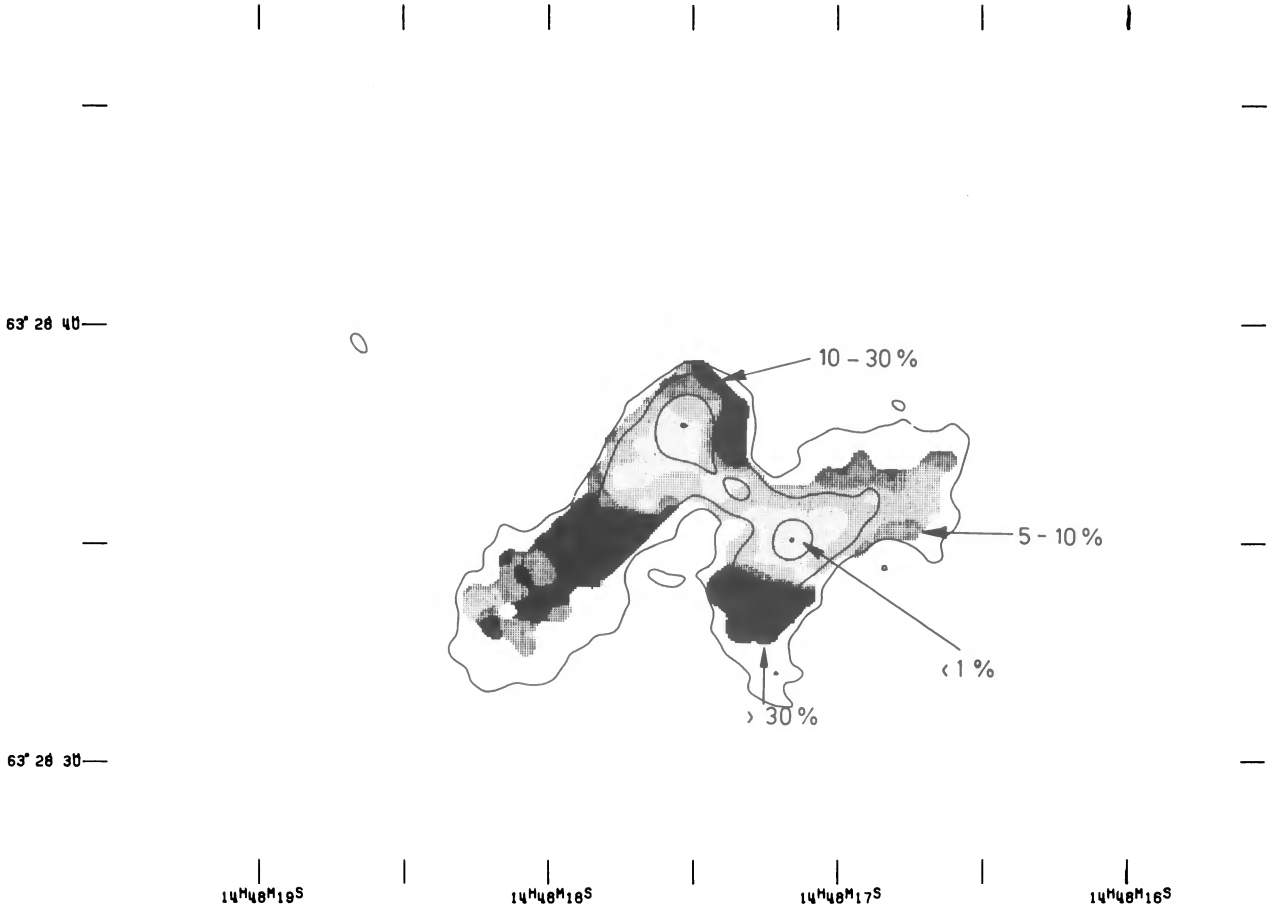

FIG. 3.—Percentage polarization at 6 cm shown in gray-scale form with the values indicated in the figure. The 6 cm total intensity contours are at 1, 4, and 30 mJy per restoring beam. The scale and orientation are as in Figs. 1*a* and 2.

$\gtrsim 30\%$. Note that the region of lowest polarization coincides almost (but not exactly) with the brightest regions of total intensity.

Recent multifrequency mapping of 3C 305 at the VLA at 1.4, 5, and 15 GHz shows that the percentage polarization increases strongly with frequency throughout the source. This behavior is characteristic of nonthermal radio radiation which has suffered Faraday depolarization. A detailed comparison of these multifrequency maps will be deferred to a future paper (Miley *et al.* 1982).

As a rough estimate of the densities required for Faraday depolarization of the bright part of the source, we take the product of the rotation measure through the source and the square of the wavelength as exceeding 180°. We can then write $n_e H_{\parallel} \phi_p L \times (6 \text{ cm})^2 \gtrsim \pi$, where $H_{\parallel}$ is the parallel magnetic field, and $L\phi_p$ is the effective path length through the depolarizing region written in terms of the total path length through the radio source (L) and the filling factor of the depolarizing thermal plasma (ϕ_p). Taking magnetic field strengths corresponding to the minimum energy situation gives the limit on $n_e\phi_p$ also listed in Table 6.

Note that the inferred magnetic field is circumferential along the north and west edges of the radio lobe B and is directed along the faint extensions B′ and A″.

b) Optical Imaging

i) *Distribution of Line-Emitting Gas*

Figure 4 shows a contour representation of the image of the Hα plus [N II] $\lambda\lambda$6548, 6584 line-emitting gas with the continuum removed (hereafter referred to as the "Hα image"). The Hα image has been displayed superposed on a gray-scale representation of the radio percentage-polarization distribution. There is a remarkable *similarity between the emission-line and radio continuum structures*. Both exhibit bright "lobes" near the nucleus, leading to fainter arms further out.

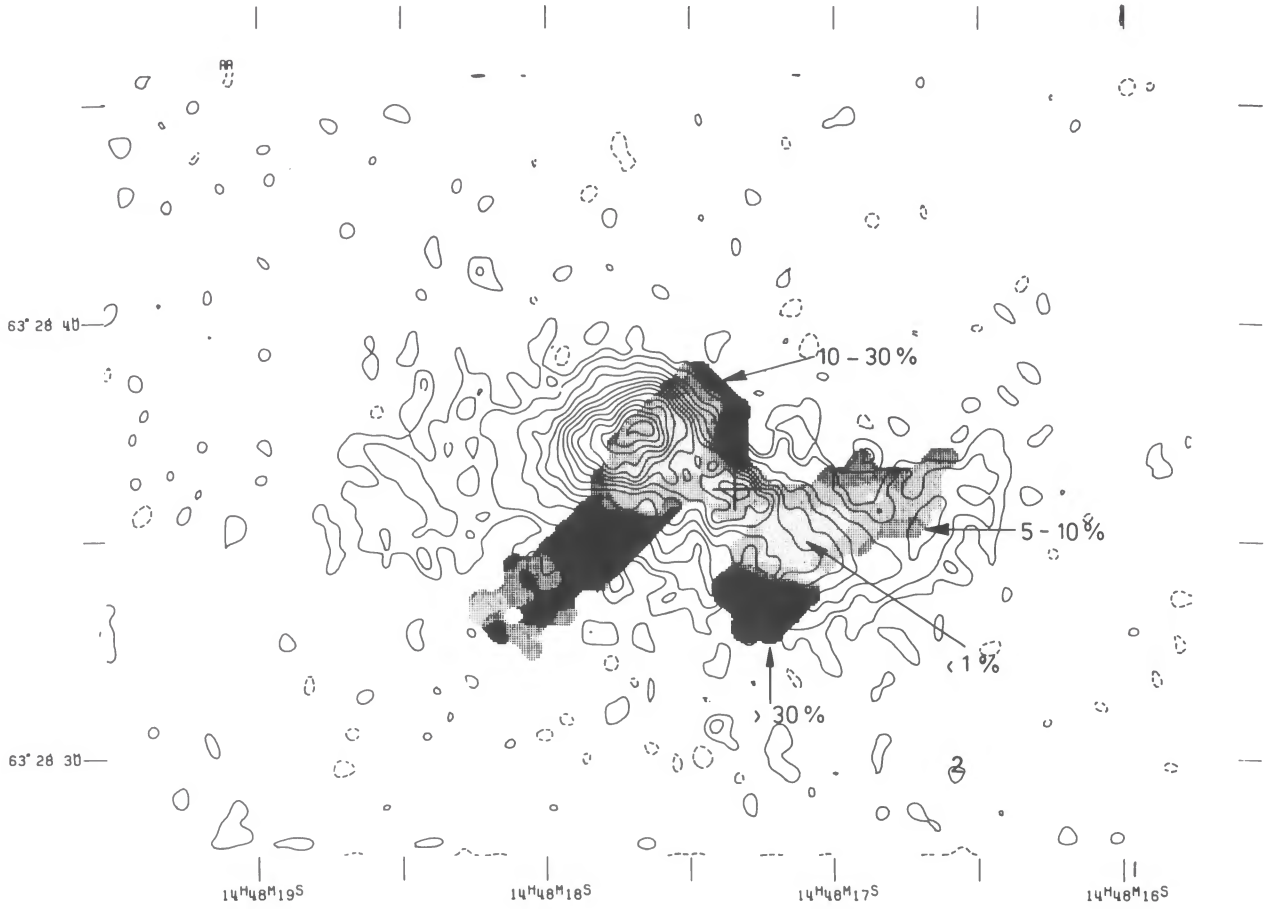

FIG. 4.—The 6 cm percentage polarization in gray scale (as in Fig. 3) superposed on a contour plot of the intensity distribution of the Hα + [N II] $\lambda\lambda$6548, 6584 emission lines with the stellar continuum removed. The contours for the emission-line gas are (in arbitrary units of surface brightness) at levels of -0.4 (*dashed*), 0.4, 0.8, and then in steps of 0.8 up to 16.8.

The principal axis defined by the bright Hα lobes (Table 3) is $53 \pm 4°$. This is very close to the orientation of the radio jet ($54° \pm 2°$), but is significantly offset by some 10° from the axis of the radio lobes (43°). Moreover, the emission-line arms lie adjacent to but do not coincide with the radio arms. Finally, while the radio source is very "narrow" in the region of the lobes (width ≤ 250 pc), the emission-line gas is extended by ~ 2 kpc perpendicular to its principal axis to the southeast (it appears unresolved in the transverse direction to the northwest). We conclude that there are important differences as well as similarities between the morphologies of the gas and radio source.

In addition to the morphological similarities there is also a detailed *anticorrelation between the presence of the line emission and the percentage radio polarization*. This suggests that the gas that is emitting the lines is closely associated with the thermal medium that depolarizes the radio emission.

Our [O III] λ5007 image (not shown) is very similar to the Hα image, except that the arms are $\sim 75\%$ stronger relative to the nucleus than in the Hα image, while the bright NE lobe is a factor of 2 weaker. A more detailed discussion of spatial variations in the relative line strengths will be given below. From this discussion, we will conclude that the morphology of the gas in the light of different emission lines is qualitatively similar to Figure 4.

ii) *Galaxy Morphology*

The unusual optical morphology of the parent galaxy of 3C 305 is discussed in detail by Sandage (1966). We list here the principal salient conclusions from his investigation, all of which are fully supported by our own data. For the convenience of the reader, we display our *V* band image of 3C 305 in contour form in Figure 5.

1. The main body of the galaxy is an ellipsoid with a major axis in P.A. $\sim 75°$. Sandage's photograph shows the main body to be extended $\sim 22 \times 12$ kpc ($\sim 27'' \times$

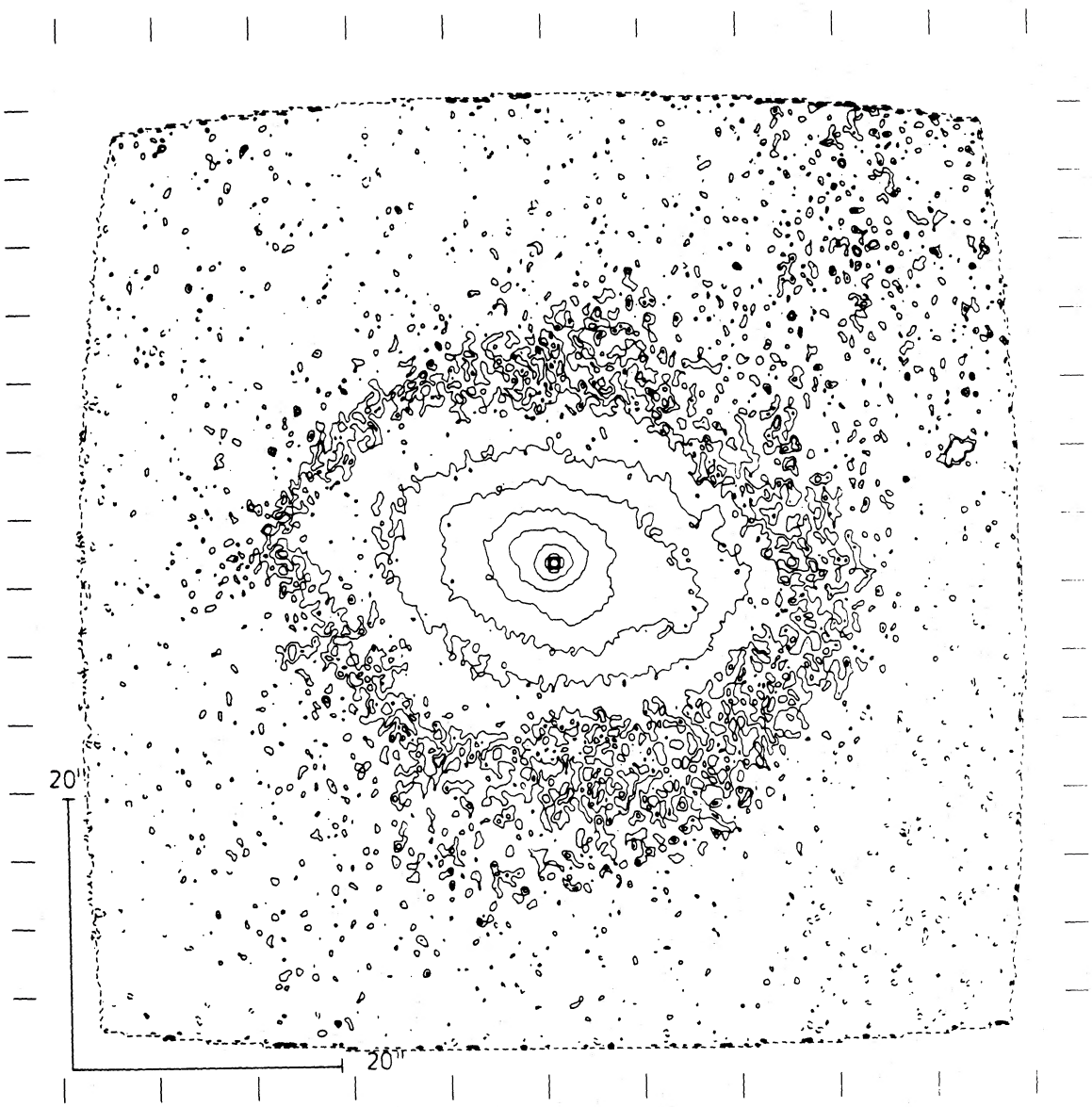

FIG. 5.—A contour plot of the intensity distribution of 3C 305 obtained with the Video Camera through a standard *V*-band filter. The scale is indicated in the figure which is oriented with north on the top and east to the left. Contours are (in arbitrary units of surface brightness) at levels of −2 (*dashed*), 2, 6, 14, 30, 62, 126, 254, 510, 1022, 2046, and 4094.

15″), while we can trace it farther out, finding a maximal extent of ~33×21 kpc (~40″×25″).

2. West of the nucleus, the ellipsoid is crossed obliquely by a thin dust lane in a P.A. ≈120°. The dust lane passes through (in projection) the SW radio lobe.

3. A "veil of obscuration" consisting of mottled dust patches can also be seen, concentrated largely to the south and west of the nucleus. This, together with the location of the dust lane, leads Sandage to identify the south as the near side of the galaxy.

4. A single faint "spiral arm," which unwraps in the clockwise direction, extends over ~35×45 kpc (~42″×55″). The inner part of this feature seems to connect to the oblique dust lane.

5. The combination of a spiral-arm–like feature and the presence of dust are the criteria used by Sandage to classify 3C 305 as an Sa or Sa pec. Classifications as E4 pec or S0 pec seem equally likely.

6. The absolute magnitude (Sandage 1966) of the galaxy is $M_v = -22.61$ ($M_B = -21.84$), so that both in terms of size and luminosity 3C 305 is a very large and luminous galaxy (Hoessel, Gunn, and Thuan 1980 find $M_v = -22.2 \pm 0.35$ for first-ranked cluster galaxies adjusted to $H_0 = 75$ km s^{-1} Mpc^{-1}).

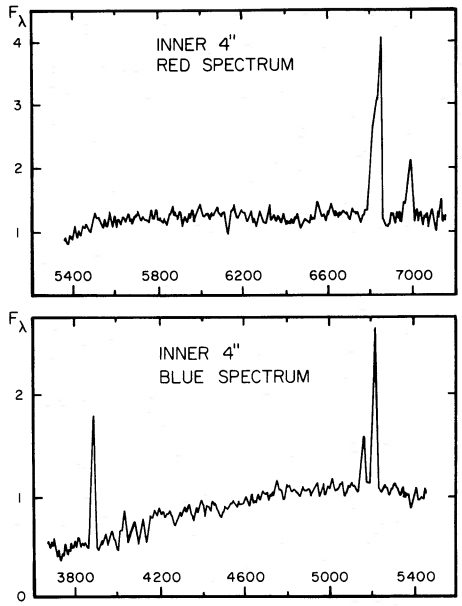

FIG. 6.—Spectra obtained with the IIDS through a 4″ circular aperture centered on the nucleus. The observed wavelength scale is indicated, and the blue and red spectra are plotted separately in arbitrary units of flux per wavelength (F_λ). Note that the vertical scales in F_λ are different for the two spectra.

c) *Optical Spectroscopy*

The spectrum of the nuclear region obtained through a 4″ circular aperture is shown in Figure 6, and the spatial variations in the relative emission-line ratios from our slit spectra are shown in Figure 7. The strengths of the most prominent stellar absorption features and emission lines in the nucleus are given in Tables 7 and 8, respectively.

TABLE 7

ABSORPTION-LINE EQUIVALENT WIDTHS IN INNER 4″ OF 3C 305

Line	E.W. (Å)
Na D λ5892	5.1±0.3
Mg I λ5174	3.4±0.4
CH G band λ4300	5.9±0.9
Hδ	4.5±0.4
Ca II K λ3934	7.1±0.2
H8	5.0±1.0
H9	6.8±1.3

i) *Stellar and Nonthermal Components*

The most striking aspects of the stellar spectrum are the presence of relatively strong Balmer absorption lines and a rather blue continuum. Note that Sandage (1966) also gives a relatively blue value of $B-V=0.76$ for 3C 305. These features are not typical for an early-type galaxy such as 3C 305 and are almost certainly produced by a component of young (age $\ll 10^{10}$ yr) stars mixed with the dominant old population (cf. Heckman 1980*a*). Gas and dust (out of which such stars could have formed) are obviously available in 3C 305.

The lack of strong variation in the stellar spectrum along our slit positions means that this component of young stars is distributed throughout the bright part of the galaxy.

The stellar spectrum of 3C 305 bears a strong resemblance to that of the nucleus of M51 (Heckman, Balick, and Crane 1980). We can therefore estimate the rate of star formation, using the population synthesis model constructed by Turnrose (1976) for the M51 nucleus. Scaling this model up to the luminosity of

TABLE 8

RELATIVE EMISSION-LINE STRENGTHS IN INNER 4″ OF 3C 305

Line	$F/F_{H\beta}$	$I/I_{H\beta}$[a]	Seyfert 2[b]	NGC 1052[c]
[S II] λ6731	2.4	1.0	0.8	1.3
[S II] λ6717	2.4	1.0	0.8	1.7
[N II] λ6584	10.1	4.4	2.3	3.0
Hα	6.8	2.9	2.9	2.9
[N II] λ6548	3.4	1.5	0.8	1.0
[O I] λ6300	0.9	0.4	0.5	1.5
[O III] λ5007	6.4	5.9	11.0	2.2
[O III] λ4959	2.1	2.0	3.7	0.8
Hβ	≡1.0	≡1.0	≡1.0	≡1.0
[Ne III] λ3869	0.5	1.1	1.5	0.6
[O II] λ3727	5.3	14.0	3.0	8.0

[a] De-reddened with $E_{B-V}=0.85$.
[b] Composite spectrum from Koski 1978.
[c] From Fosbury *et al.* 1978. Typical shock-heated LINER (Heckman 1980*b*).

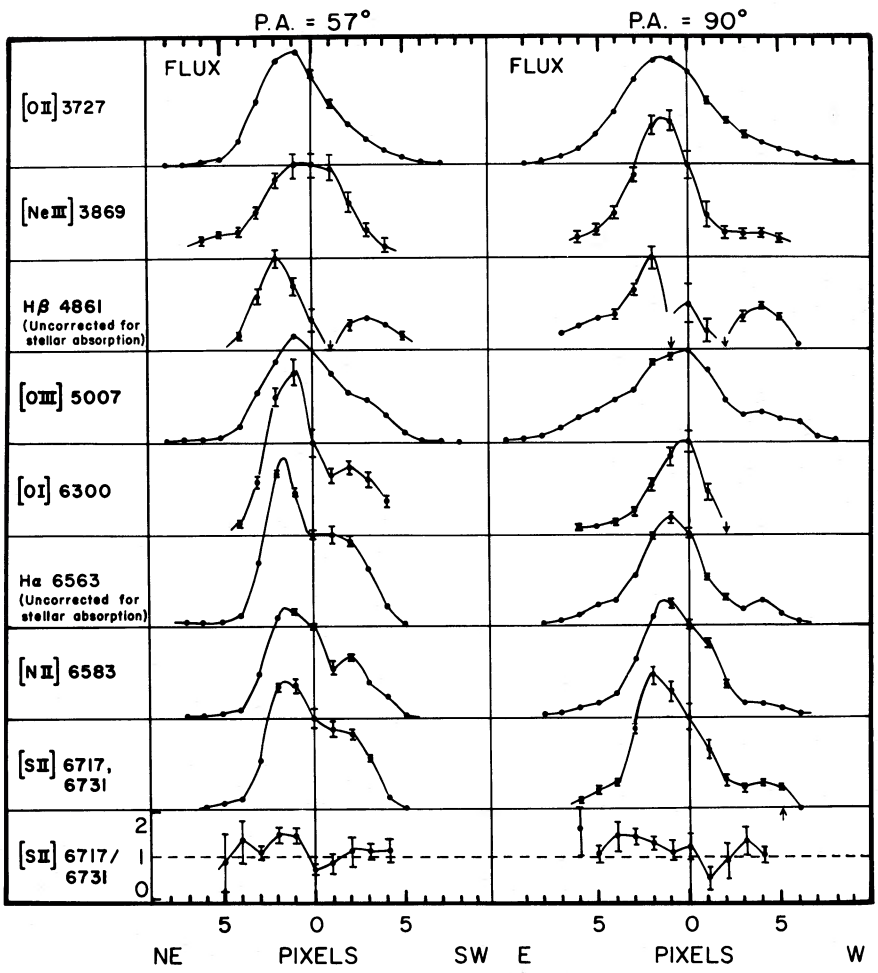

FIG. 7.—The variation in relative emission-line strength along the two slit positions covered (P.A. = 57°, 90°). The vertical axis for each plot is normalized to the total line flux per spatial pixel at the position of the nucleus. Note that the effects of stellar Hα and Hβ absorption lines have *not* been removed from the respective plots (but *have* been removed from the relative intensities listed in Table 6). The density-sensitive intensity ratio of [S II] λ6717 to λ6731 is also indicated. The horizontal scale is in units of pixels (= 1".3) relative to the nucleus.

3C 305 indicates that over the last $\sim 10^9$ years stars have formed at the rate of $\sim 3\ M_\odot$ per year, or at more than three times the rate found for a normal early-type galaxy of comparable luminosity (Faber and Gallagher 1976).

Yee and Oke (1978) attempted to deconvolve the optical continuum of the inner 10" of 3C 305 into a stellar spectrum (typical of an elliptical galaxy) and a nonstellar, featureless power-law component. Their results indicated that 5–9% of the continuum at λ5460 was nonstellar. However, we have seen that the stellar continuum of 3C 305 is not that of a typical elliptical galaxy but is "contaminated" by the contribution of relatively young and hence relatively blue stars. Thus Yee and Oke have probably significantly overestimated the nonstellar contribution.

ii) *Emission-Line Intensities*

Several conclusions can be drawn about the characteristics of the emission-line spectrum and its spatial variation. These are described below and summarized in Table 9.

1. *Ionization state.*—The spectrum is characterized by strong forbidden lines from a wide range of ionization states (e.g., O^0, O^+, O^{++}, Ne^{++}, etc.). Heckman (1980*b*) and Baldwin, Phillips, and Terlevich (1981) have devised schemes for classifying the emission-line spectra of active galaxies. Based on their precepts, the spectrum of 3C 305 bears little resemblance to that of either an ordinary H II region or a planetary nebula (e.g., to gas photoionized by hot stars). Instead, the spectrum is intermediate between that of a Seyfert

TABLE 9

SOME APPROXIMATE PARAMETERS OF THE EMISSION-LINE GAS

	Lobes	Arms
Luminosity, L_{Em} ...	10^{44} ergs s^{-1}	$10^{43.5}$ ergs s^{-1} [a]
Density, n_e	10^3 cm^{-3}	$\lesssim 10^{2.5}$ cm^{-3}
Mass, M_{Em}	$10^7\ M_\odot$	$\gtrsim 10^7\ M_\odot$ [a]
$\phi_{Em}\, n_e$	$2.5\text{–}16\times 10^{-2}$	...
Temperature, T_e	10,000–40,000 K	$\sim 10^4$ K?
Thermal pressure ...	10^{-8}–10^{-9} dyn cm^{-2}	$\lesssim 10^{-9.5}$
Kinetic energy	$10^{55.5}$ ergs s^{-1}	$\gtrsim 10^{55}$ ergs s^{-1} [a]

[a]Assuming $E_{B-V} \approx 0.85$ (§ III) in the arms as well as in the lobes.

nucleus (Koski 1978; Osterbrock 1977), in which the lines of highly ionized species are relatively strong, and the spectrum of a low-ionization nuclear emission-line region (LINER) observed in the nuclei of many nearby early-type galaxies (Heckman 1980*b*).

The spatial variations in the relative emission-line strengths are shown in Figure 7. Because no relative flux calibration has been attempted for the slit spectra, all line intensities are normalized to their nuclear values. A few conclusions can be drawn from Figure 7. (*a*) All emission-line fluxes peak at or near the eastern lobe. While the distributions of the emission lines differ in detail, their general distributions are probably similar to the Hα+[N II] image in Figure 5. (*b*) The low ionization lines (i.e., [O I] λ6300, [S II] $\lambda\lambda$6717, 6731, [O II] λ3727, and [N II] λ6584) are more concentrated toward the bright Hα lobes than are the higher ionization lines [O III] λ5007 and [Ne III] λ3869. The lobes are hence characterized by a lower overall degree of ionization than the arms. (*c*) The violet lines are relatively weak to the WSW of the nucleus in a way that is consistent with reddening produced by the dust lane and dust patches that are located in this part of the galaxy (cf. Sandage 1966).

2. *Temperature.*—We have determined a limit for the electron temperature of the gas near the NE Hα lobe of $T_e \leq 25{,}000$ K using the [O III] λ4363-to-λ5007 intensity ratio. Since this limit reflects our ability to adequately subtract the stellar continuum near λ4363, our limits to T_e are significantly higher ($T_e \leq 40{,}000$ K) in the nucleus, where the emission-line equivalent widths are smaller.

3. *Density and pressure.*—The ratio of [S II] λ6717 to λ6731 was used to estimate electron densities (n_e) throughout the emission-line region. These estimates are uncertain not only because of the limited signal-to-noise ratio in the data but also because ambiguities are introduced in the de-blending procedure by the kinematic complexity of the gas near the nucleus and the lobes (see below). Because of this complexity, two pairs of Gaussians were sometimes required to de-blend the [S II] lines. Another limitation to our density estimate is its insensitivity to gas with $n_e \gg 10^4$ cm^{-3}, since the [S II] lines will be heavily quenched by collisions in such dense gas. Moreover, there is no certainty that the densities in the [S II]-emitting gas are representative of other ionization zones in the emission-line gas.

Our data show evidence for spatial variations in n_e, with the value being $\sim 10^{3.2\pm0.4}$ cm^{-3} in the nucleus, $10^{2.5\pm0.3}$ cm^{-3} near the eastern lobe, $10^{3.3\pm0.3}$ cm^{-3} near the western lobe, and $\lesssim 10^{2.5}$ cm^{-3} in the arms. In light of the observational and interpretive uncertainties discussed above we will take $n_e \approx 10^3$ cm^{-3} as a representative value for the bright regions (nucleus and lobes) and $n_e \lesssim 10^{2.5}$ cm^{-3} for the arms.

Taking $n_e \approx 10^3$ cm^{-3} and $T \approx 2\times 10^4$ K implies a gas pressure of $\sim 10^{-8.5}$ dyn cm^{-2} for the emission-line gas.

4. *Reddening.*—The ratio of the Hα to Hβ fluxes near the nucleus is 7 ± 1. This quantity is difficult to measure accurately because of the uncertain correction for the effects of the stellar Balmer absorption features. If the intrinsic emission-line spectrum is taken to be that of Case B recombination (Osterbrock 1974), as Koski (1978) and others have argued is the case for the narrow emission lines in Seyfert galaxies, a value for $E_{B-V} \approx 0.85\pm0.15$ is implied. Such a large value is not unreasonable since $\sim 30\%$ of the Seyferts studied by Koski had E_{B-V} as large or larger. Moreover, as described above, the galaxy has a very dusty appearance. We cannot, however, rule out the possibility that the *intrinsic* Hα/Hβ ratio is rather large in 3C 305 due to the effects of collisional excitation or Balmer self-absorption (e.g., Netzer 1981). In such a case the true value for E_{B-V} could be appreciably smaller than 0.85.

5. *Luminosity.*—The spectrophotometric data of Yee and Oke (1978), together with our spectroscopic data, indicate an Hα flux of 7.6×10^{-14} ergs cm^{-2} s^{-1} or an apparent Hα luminosity $L_{H\alpha} \approx 2.4\times 10^{41}$ ergs s^{-1}. Taking our derived value of $E_{B-V} = 0.85$ at face value, the intrinsic $L_{H\alpha} \approx 3\times 10^{42}$ ergs s^{-1}. From our emission-line spectrum and assuming standard Case B conditions, we derive a total intrinsic emission-line luminosity of $L_{EL} \approx 10^{44}$ ergs s^{-1}.

6. *Mass and kinetic energy.*—To produce the above Hα luminosities, a mass of ionized hydrogen $M_{H^+} \approx 1\text{–}2 \times 10^{10} n_e^{-1}\ M_\odot$ is required (for $T_e = 1\text{–}2\times 10^4$ K). Taking $n_e \approx 10^3$ cm^{-3} in the bright part of the gas (which assumes that the densities over the entire thermal region are the same as those measured in the S^+ zone) implies $M_{H^+} \approx 1\text{–}2\times 10^7\ M_\odot$.

Taking $M_{H^+} = 1.5\times 10^7\ M_\odot$ and a velocity of 300 km s^{-1} as characterizing the bright region of the emission-line gas would imply a kinetic energy for the gas of 1.5×10^{55} ergs, which is very similar to the minimum energy in the bright radio lobes (Table 6).

7. *Clumpiness.*—Taking $M_{H^+} \approx 1.5\times 10^7\ M_\odot$ and $n_e \approx 10^3$ cm^{-3} and the measured size of the bright part of the emission-line region (~ 2 kpc wide $\times \sim 6$ kpc

long $\times t$ kpc thick), we derive a filling factor for the emission-line gas $\phi_e \approx 5 \times 10^{-5}\, t^{-1}$. Thus, for a cylindrical geometry ($t \approx 2$ kpc) $\phi_e \approx$ a few times 10^{-5}, while if the gas is confined to a disk comparable in thickness to that in our own galaxy ($t \approx 0.3$ kpc) $\phi_e \approx 10^{-4}$. The emission-line gas is evidently highly clumped.

iii) *Emission-Line Velocities*

The best data for studying the kinematics of the emission-line gas are the high (~ 130 km s^{-1}) resolution spectra in the vicinity of the [O III] λ5007 line (see Table 5). Such spectra were taken at P.A. 57° (close to the fundamental emission-line and radio axes), 100° (through the brightest parts of the Hα arms), and 150° (close to the galaxy minor axis at 165°). These high resolution data are shown in contour form in Figure 8 and as row plots in Figure 9. The center velocities and line widths fitted to the data are shown in Figure 10. The kinematic description which follows is entirely consistent with the lower dispersion data summarized in Table 5.

1. *Velocities.*—The nucleus of the galaxy is the center of symmetry for the kinematics of the gas. Relative to the nucleus, the gas to the east is approaching, while the gas to the west is receding. The radial velocities increase almost linearly to about ± 260 km s^{-1} at the edge of the Hα lobes and then may decrease slowly out to projected distances of ~ 10 kpc.

Isovelocity contours indicate that the largest velocity gradient occurs in P.A. $\sim 70 \pm 15°$, or close to the major axis of the main ellipsoidal stellar distribution at 75° (see Fig. 5).

2. *Profiles.*—The emission lines are *widest* in the bright part of the emission-line region (e.g., close to the strong radio emission). Here the [O III] lines are 500–800 km s^{-1} (FWHM) wide and show a "blue wing" near the base of the line profile clearly extending to ~ 2000 km s^{-1}. The centroid of this blue wing is offset from the peak of the profile by ~ -400 km s^{-1}.

The line profiles are *complex* throughout this region and cannot be well fitted with a single Gaussian. In contrast, the gas in the Hα arms is far more quiescent (lines are often unresolved at 130 km s^{-1} resolution).

There is evidence for *differences in line width* between the various atomic species in the bright central emission-line region. Near the stellar nucleus, the various lines—[S II], [N II], [O III], [Ne III], Hα, [O II], and [O I]—have respective widths of 450 ± 50, 490 ± 60, 620 ± 70, 780 ± 120, 800 ± 80, 850 ± 80, and 1300 ± 200 km s^{-1} (FWHM). The errors are inferred from comparisons of the widths measured in the various slit positions. Near the eastern lobe, the various line widths are all near 600 km s^{-1}, with the possible exceptions of the [Ne III] line (470 ± 140 km s^{-1}) and [O II] line (740 ± 70 km s^{-1}). The narrowness of [Ne III] relative to [O II] in the lobe has been confirmed by high-resolution spectroscopy. Variations of line width with species have been noted before in active nuclei (Pelat, Alloin, and Fosbury 1981; Osterbrock 1981; Balick and Heckman 1979).

IV. DISCUSSION

a) Emission Line / Radio Source Relationship

Any discussion of either the radio source or the emission-line gas in 3C 305 must take into account the following relationships which exist between the two regimes drawn from the figures and by comparison of Tables 6 and 9.

1. There is a strong *morphological* resemblance between the gas and the radio source (the size and orientation of both the principal and secondary structure).

2. There is a clear anticorrelation between the presence of the emission-line gas and the fractional *radio polarization*.

3. The *kinematics* of the emission-line gas are disturbed and complex in those regions closest to the bright radio emission. A statistical correlation between emission-line widths and the power of kiloparsec-sized nuclear radio emission has been noted previously for a large sample of Seyferts and radio galaxies (Wilson and Willis 1980; Heckman *et al.* 1981). The present results, which indicate a connection between line width and radio power *within an individual galaxy*, are further evidence that in active galaxies the presence of relativistic particles and the kinematics of the emission-line gas are closely related.

4. The thermal *pressure* in the emission-line lobes is similar to the minimum-energy internal pressures given in Table 6 for the radio lobes. This suggests that the clumpy emission-line gas is in rough pressure balance with the radio plasma. Such a situation could occur if the thermal gas were imbedded in the relativistic plasma or if both were in pressure balance with a third, omnipresent medium.

5. The *kinetic energy* of $\gtrsim 1.5 \times 10^{55}$ ergs derived for the bright regions of the gas is very similar to the (minimum) energy in the bright part of the radio source (2–3×10^{55} ergs). This is evidence that within 3C 305 there is a rough equipartition of energy between the emission-line and relativistic media, as Wilson and Willis (1980) have argued is the general case in Seyfert nuclei with kiloparsec-sized nuclear radio sources.

The radio luminosity from 10 MHz to 100 GHz ($\sim 10^{42}$ ergs) is similar to the *kinetic energy flux* through the emission-line region (i.e., the total kinetic energy of the gas divided by the time for a cloud to leave the region). Note that the total calculated radio luminosity is not very sensitive to the choice of cutoff frequencies.

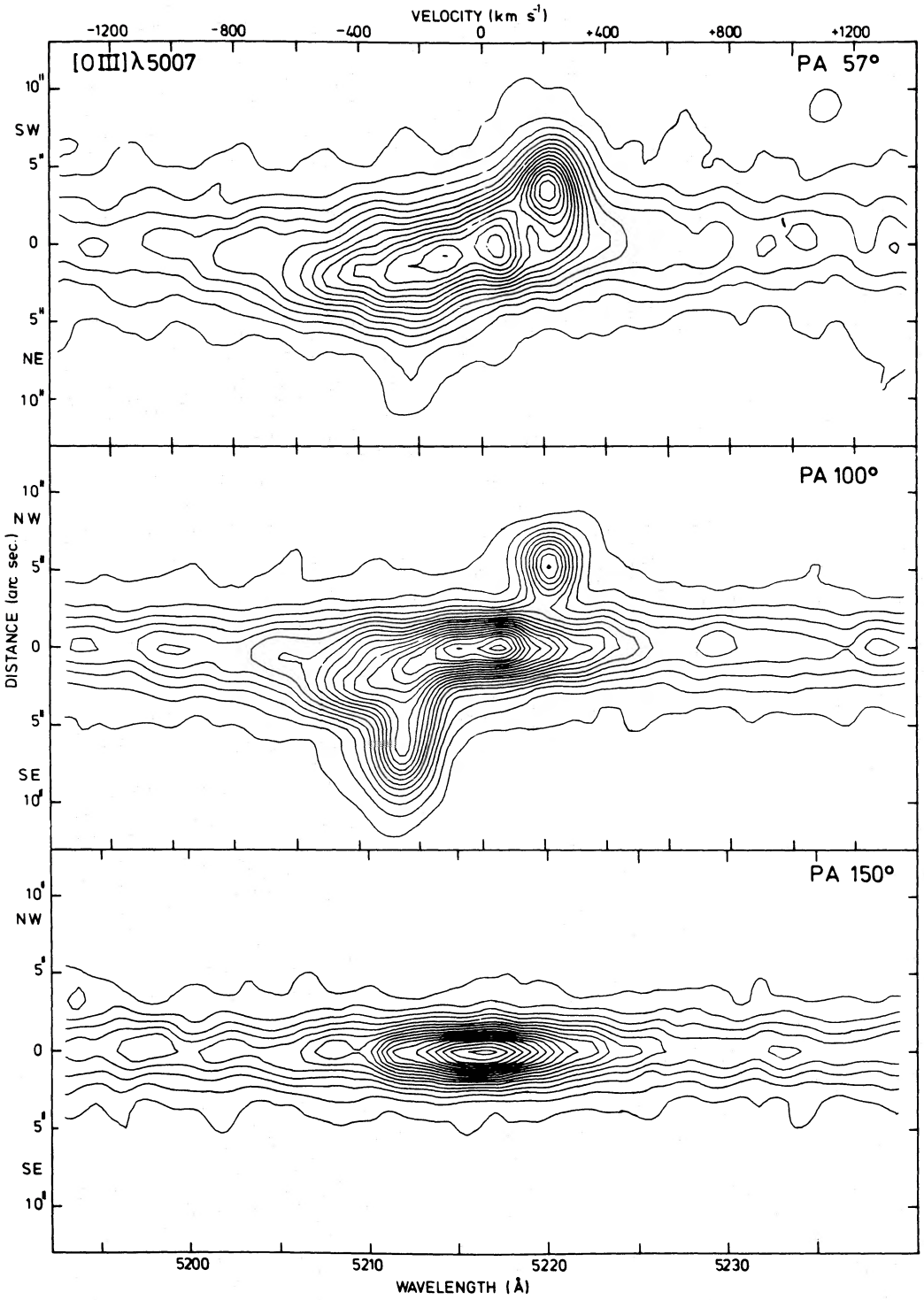

FIG. 8.—Contour plots of the high-resolution (FWHM = 2.2 Å ≈ 125 km s^{-1}) slit spectra in the vicinity of the [O III] λ5007 line along the three P.A.'s covered. The contours are at linear intervals of 50 counts pixel^{-1}.

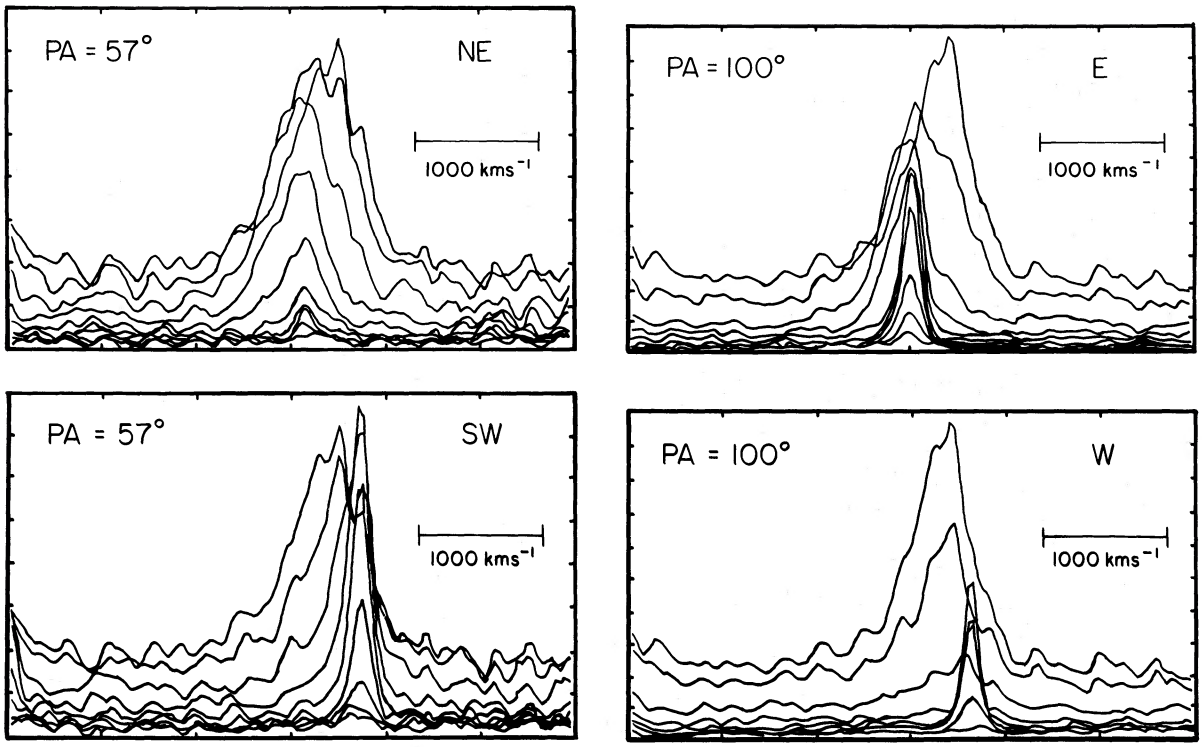

FIG. 9.—Row plots of the high-resolution (FWHM ≈ 2.2 Å) slit spectra along P.A. 57° and 90° in the vicinity of the [O III] λ5007 line. In each of the four figures the row with the highest continuum flux delineates the nucleus, and adjacent rows are located successively 1 pixel (= 1″.3) further from the nucleus in the direction indicated in the figure. The velocity scale is indicated by the horizontal bar in each figure.

b) The Line-emitting Gas

i) *Kinematics*

Because of the connection of the line-emitting gas with the radio source, it is of particular interest to discuss the kinematics of the gas in detail. The velocity field presented in § III*c* (iv) leads us to consider three possible models for the kinematics—namely, pure rotation, pure outflow, and rotation combined with outflow.

1. *Pure rotation.*—This model is supported by (1) the similarity of Figure 10 to the rotation curves of early-type galaxies (Rubin, Ford, and Thonnard 1978); (2) the alignment of the apparent rotation axis (P.A. = 160 ± 15°) and the galaxy minor axis (~165°), and (3) the evidence for a similarity between the velocity fields of the gas (Fig. 10) and the stars (Heckman *et al.* 1982).

On the assumption of rotation, the value of the radius at which solid-body rotation ends is $r_{\rm peak} \approx 2$–3 kpc, and the rotation velocity at this point is $V_{\rm peak} \approx 260(\sin i)^{-1}$ km s^{-1}. The mass within $r_{\rm peak}$ is $M_{\rm Inner} \approx 5 \times 10^{10}(\sin i)^{-2}\ M_\odot$, while the total virial mass out to $r = 8$ kpc is $M_T \approx 1.3 \times 10^{11}\ (\sin i)^{-2}\ M_\odot$, yielding a mass-to-light ratio $M_T/L_B \geq 3$ in solar units (using the value for the total L_B derived by Sandage 1966 adjusted to $H_0 = 75$ km s^{-1} Mpc^{-1}). The values for $V_{\rm peak}$, $r_{\rm peak}$, M_T, and M_T/L_B are normal for a luminous early-type disk system (Farber and Gallagher 1979; Rubin, Ford, and Thonnard 1978).

A further argument in favor of the rotation picture is that the turnover in the rotation curve at $r_{\rm peak}$ occurs near the edges of the Hα lobes. The straight inner bright region of emission-line gas would then occur in a region of solid-body rotation, whereas the Hα arms would lie in a zone of strong differential rotation where linear features are rapidly sheared into spirals. The rotation model would therefore explain the relationship which appears to exist between the spatial morphology and kinematics of the Hα/radio structure.

2. *Outflow.*—Heckman *et al.* (1981) have presented evidence that the gas in the narrow-line region of active nuclei is flowing predominantly outward and is coupled in some way to the associated radio source. Graham and Price (1981) and Miley *et al.* (1981) have presented similar evidence in the cases of the classical double radio sources Centaurus A and 3C 277.3 (Coma A), respectively. Thus, in the case of 3C 305, where the near-nuclear gas is morphologically connected with the (presumably outflowing) radio source and in which the emission-line width is closely correlated with the presence of the radio lobes, an outflow interpretation of the kinematics should be considered.

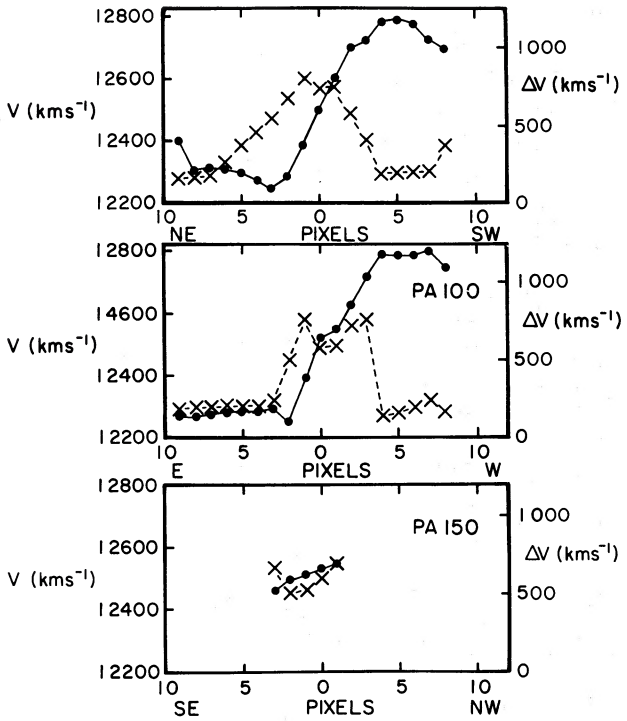

FIG. 10.—The velocity and width (FWHM) of the [O III] λ5007 line as a function of position along the three-slit position angles covered. The velocity, V, is indicated by solid dots connected by solid lines, and the line width, ΔV, is indicated by crosses connected by dashed lines. The horizontal scale is in all cases given in pixels (1".3) with respect to the nucleus.

At least two types of outflow are plausible:

a) *Outflow along the radio source axis.*—The morphological similarity between the radio source and the emission-line gas suggests that gas may be flowing along the principal radio-source axis. Although, as we have seen, the position angle of the largest velocity gradient in the gas ($70 \pm 15°$) is consistent with rotation around the galaxy's minor axis, it is not completely inconsistent with ejection close to the radio axis ($43 \pm 1°$ for the lobes, $54 \pm 5°$ for the inner jets). Moreover, the inner radio jet appears to point toward the regions of peak intensity in the Hα lobes.

There are three problems with this picture, however. First, Sandage (1966) has identified the southern part of the galaxy as the near side (based on the concentration of dust absorption features to the south). *If the emission-line gas is roughly coplanar with the dusty disk*, then the fact that the southern Hα arm is redshifted in velocity relative to the nucleus would require the gas to be flowing *inward* in a radial flow model. However, the relative geometry of the dust and emission-line gas is uncertain.

Second, preliminary results (Heckman *et al.* 1982) indicate a similarity between the stellar and gaseous kinematics, which would be a fortuitous circumstance if the dynamics of the two components were totally different.

Finally, the relative emission-line velocities continue to increase out to $\sim 4''$ from the nucleus or more than twice as far out as the edge of the radio lobes. This would be difficult to understand if the gas was being accelerated out by the radio source. On the other hand, as we shall discuss below, the existence and morphology of the Hα arms is indirect evidence that the emission-line gas may have a component of motion along the radio axis. These arms might represent material which has been accelerated outward during its passage through the jet, and which subsequently interacts with disk gas beyond the point at which the radio plasma is braked.

b) *Outflow away from the radio source.*—Outflow transverse to the radio source axis is suggested by several aspects of our data: (i) A blueward asymmetry in the [O III] λ5007 line profile is seen throughout the kinematically disturbed region near the radio source. The general occurrence of blue asymmetries in the global [O III] line profiles of active nuclei has been interpreted (Heckman *et al.* 1981) as evidence that gas and dust are mixed together and flowing outward. In the case of 3C 305 we would suppose that the receding gas on the back of the radio source is more effectively hidden by dust than the approaching gas on the front side. (ii) There is a close connection between the kinematically disturbed portion of the emission-line region and the radio source. (iii) The size of the emission-line region in the direction perpendicular to the radio-source axis is larger than the corresponding breadth of the radio source.

3. *Rotation plus outflow.*—The above discussion indicates that the kinematics of the gas are complex and strongly suggests that a hybrid model combining rotation with outflow be considered. A *rotational* component could account for most of the large-scale velocity gradients, motion *away from the radio source* could explain the broad asymmetric line profiles near the radio lobes, while a component *along the radio axis* might be responsible for the Hα arms. Such a model would be plausible since, if the radio source is indeed an inhomogeneous beam traveling supersonically through a rotating disk of gas, a complex hydrodynamical situation would result in which some gas would be heated and would subsequently expand away from the radio source while other gas would be entrained in the advancing jet.

This model, which is somewhat similar to the model proposed for NGC 4258 by van der Kruit, Oort, and Mathewson (1972), would have most of the advantages of pure rotation or pure outflow models. For example, the reasonable values for the mass and M_T/L_B implied by the pure rotation model were derived mainly from

the kinematically quiescent outer emission-line arms and would also apply to this hybrid model.

ii) *Ionization*

Several processes could contribute to ionizing the line-emitting gas, some of which depend on the presence of the radio source. We shall consider each of them in turn.

1. *Photoionization by hot stars.*—Using the criteria of Baldwin, Phillips, and Terlevich (1981) and of Heckman (1980*a*, *b*), we find that the relative emission-line strengths in 3C 305 lie well outside the domain of gas photoionized by hot stars. Even allowing for the presence of relatively young stars in 3C 305, such a mechanism could play only a minor role in ionizing the gas.

2. *Photoionization by a central nonthermal source.*—This is the mechanism thought to be the source of ionization in most active nuclei (e.g., Yee 1980; Shuder 1982), but there are major problems with this model for 3C 305.

First, there is no evidence for such a continuum (§ III*c*[ii]). Second, the relatively small amount of spatial variation seen in the relative strengths of the emission lines of the high and low ionization species would require that the so-called ionization parameter (the local ratio of photon density to gas density) must vary by less than a factor of ~ 2 throughout the 3C 305 emission-line region (cf. Ulrich and Péquignot 1980). For this to occur, the gas density must fall nearly as the square of the distance from the nucleus, which is not supported by our data on n_e (§ III*c*[iii] (2)). Third, of some 35 active galaxies for which images of the emission-line gas have been obtained (Balick and Heckman 1982*a*), 3C 305 is the only case in which the line intensities do not peak strongly at the nucleus.

3. *Photoionization by an extended nonthermal source.*—Such a source could be the high-energy continuation of the radio synchrotron spectrum, as observed in the Crab Nebula (Kirshner 1974) and in the jets of some radio galaxies (Butcher, van Breugel, and Miley 1980; Miley *et al.* 1981).

There are, however, several problems with this model: First, there is no observational evidence for a nonthermal continuum associated with the radio lobes (§ III*c*[ii]).

Second, the nonthermal continuum in the Crab Nebula and in the radio/optical jets steepens from the radio to the optical and beyond. In contrast, to produce an adequate Lyman continuum luminosity the radio-to-ultraviolet spectral index required in 3C 305 would have to be significantly flatter than the measured radio spectral index ($\alpha = 0.58$ versus 0.86, where $S_\nu \approx \nu^{-\alpha}$).

Finally, the spatial variations in the ionization state of the gas do not agree with the predictions of a simple model in which the radio-to-ultraviolet continuum is constant throughout the radio source (as Owen, Hardee, and Bignell 1980 find to be the case in the M87 jet). In particular, the gas is least highly ionized near the brightest (eastern) radio lobe. The observed spatial variations in density are not able to account for this disagreement, since n_e is apparently lower near the eastern radio lobe than it is in the nucleus or near the western lobe.

4. *Collisional ionization by fast particles.*—Ionization of the gas by particles in the low-energy ($\gamma \approx 20$) tail of the distribution of the relativistic synchrotron-emitting particles is an obvious possibility in 3C 305.

There is, however, a simple objection to this model: Most of the emission-line gas does not overlap the radio source, and there is no evidence that the ionization state of the gas declines with distance from the radio source.

5. *Ionization by shock waves.*—The large velocities observed in the emission-line clouds together with the even larger velocities inferred for the radio source (see below) imply highly supersonic motion in 3C 305. Thus, shock waves which produce both ionizing *radiation* and *collisional* ionization may be important in "energizing" the emission-line region.

The supersonic motion of the radio source will drive blast waves into the ambient medium. As the shock fronts expand away from the radio source, they will sweep up material in a manner analogous to that within a supernova remnant. The production and excitation of emission-line gas could also proceed as in a supernova remnant. Moreover, some material might pass through the radio jets and would then be accelerated outward along the radio axis. Since one would expect a range in cloud sizes and masses, these clouds would not all be accelerated at the same rate. Thus, collisions of fast and slow clouds would also occur in the vicinity of the radio source, leading to conversion of kinetic into thermal energy via shocks. Some of these outbound clouds might well travel beyond the point at which the radio source is braked. The interaction of these clouds and the ambient disk gas could conceivably ionize the regions of the Hα arms. The pronounced S shape of the arms would follow naturally from the combination of rotation and outflow in the cloud kinematics.

Collisional heating followed by roughly isobaric cooling and collapse of interstellar clouds could produce the relatively dense emission-line clouds. As the shocked clouds cool, they would radiate optical emission lines. It is likely that the surrounding hot shock-heated medium would contribute to the excitation of the emission-line gas through repressurizing shocks driven into the clouds (Cowie, Fabian, and Nulsen 1980), through production of ionizing radiation and possibly through conductive losses to the clouds. A model of this type would agree well with our conclusion above, that the morphology and kinematics of the emission-line gas is most plausibly explained in terms of a rotating disk combined with expansion away from (and possibly along) the radio axis.

However, one problem with this picture is the absence of detectable soft X-rays from 3C 305; Fabbiano (1981) finds $L_x \lesssim 10^{42}$ ergs s^{-1} in the 0.5–4.5 keV band compared with our estimate of an emission-line luminosity of $\sim 10^{44}$ ergs s^{-1}. There are two ways out of this apparent dilemma. First, most of the gas may be heated to temperatures that are either too low ($T \lesssim$ a few $\times 10^6$ K) or too high ($T \gtrsim 10^9$ K) to produce a substantial luminosity in the 0.5–4.5 keV range. The observed emission-line velocities ($\sigma \approx 250$ km s^{-1}) correspond to a kinetic temperature of $\sim 10^{6.2}$ K and shocks at 250 km s^{-1} will heat atomic gas to $\lesssim 10^{6.0}$ K (McKee and Hollenbach 1980). Gas at these temperatures would radiate strongly above the Lyman limit but only weakly in the 0.5–4.5 keV range (Raymond and Smith 1977). For 10^{44} ergs s^{-1} in ionizing radiation from gas in this temperature range, the luminosities in the [Fe XIV] λ5303 and [Fe X] λ6374 coronal emission lines would range from $< 10^{40}$ to 5×10^{41} ergs s^{-1} (Nussbaumer and Osterbrock 1970), depending strongly on temperature, compared with our limits on the (de-reddened) luminosities of both lines of $\leq 3 \times 10^{41}$ ergs s^{-1}.

The second possibility—that the soft X-ray flux is absorbed by cool gas along the line of sight—is rather unlikely, since it would require a column density $n_{\rm H} \sim 10^{23}$ cm^{-2} (Brown and Gould 1970). This exceeds by an order of magnitude the value of $n_{\rm H}$ derived from the measured extinction ($A_v = 2.5$) and the $n_{\rm H}$ versus A_v relation for our Galaxy (Gorenstein 1975).

In any event, other objects in which emission lines are probably shock-excited and in which the emission-line luminosity is *at least* an order of magnitude larger than the 0.5–4.5 keV luminosity are known to exist (some supernova remnants in M31, Kirshner 1981).

We conclude that (at present) there are no data that rule out some mixture of collisional and photoionization driven by shock waves as the dominant excitation mechanism in 3C 305. The same probably cannot be said of the other mechanisms considered above.

c) *The Radio Source*

The most widely favored models of extended extragalactic radio sources are those in which the extended lobes are powered by bulk kinetic energy of a fluid transported from the nucleus along the jet (e.g., Rees, Begelman, and Blandford 1981). In this section we shall consider 3C 305 within the context of such a viewpoint.

In our discussion we shall distinguish $V_{\rm jet}$, the bulk velocity of energy flow in the jet, from V_l, the velocity at which the leading edge of the radio lobes advances into the ambient medium. Also, where necessary, we shall assume that the energy in the radio source is $kE_{\rm min}$, where $E_{\rm min}$ is the minimum energy value derived from equipartition arguments. The agreement of the thermal pressure, the kinetic energy, and the kinetic energy flux of the line-emitting gas with the minimum energy parameters of the radio lobes which we pointed out in § IV*a* are all circumstantial evidence that the energy in the radio source is close to the minimum value ($k = 1$).

i) *Production of the Radio Emission*

We have seen that the statistics of active galaxies together with the detailed properties of 3C 305 provide convincing evidence that wider emission lines are associated with larger radio luminosities for cases in which the radio source and emission-line gas are roughly cospatial. This connection suggests that both the kinetic energy in the emission-line gas and the energy in the synchrotron-emitting plasma have a common origin.

It seems plausible that this common origin is the interaction between the bulk fluid in the jet and the ambient medium. The knots in the radio jet may well pinpoint clouds in the interstellar medium near where such processes would be enhanced. The physics of this process may be similar in some ways to the interaction of a supernova with the interstellar medium in our Galaxy. As reviewed by Chevalier (1977), most of the energy in such an interaction goes into heating and ionizing the ambient medium, with only ~ 3–10% ultimately going into the kinetic energy of the ambient medium and 1% or less into relativistic particles that are accelerated in the shocks and turbulent eddies generated in the interaction.

Our estimates of the energy budget in 3C 305 agree with this picture to the extent that radiative losses from the thermal material dominate the kinetic energy flux of the emission-line clouds or synchrotron radiation from the radio source.

ii) *Jet Velocity and Energy Supply*

Assuming the radio source to be powered by the bulk kinetic energy in the jet, we can write the total radio luminosity as

$$L_R = \tfrac{1}{2}\varepsilon \dot{m} V_{\rm jet}^2 = \tfrac{1}{2}\varepsilon \rho_{\rm jet} V_{\rm jet}^3 \sigma_{\rm jet}$$

$$= 10^{42} \text{ ergs s}^{-1},$$

where ε is the "efficiency" factor for conversion of the jet's kinetic energy to radio synchrotron radiation, $\rho_{\rm jet}$, $V_{\rm jet}$, and $\sigma_{\rm jet}$ are the mass density, velocity, and cross-sectional area of the jet, and $\dot{m}_{\rm jet}$ is the mass flow rate along the jet.

This expression then implies:

$$\left(\frac{V_{\rm jet}}{10^8 \text{ cm s}^{-1}}\right) = \left(\frac{\varepsilon \dot{m}_{\rm jet}}{3\ M_\odot \text{ year}^{-1}}\right)^{-1/2}.$$

We have argued that the kinematic energy of the jet material is likely (in some way) to power not only the radio emission but the optical line-emission as well. In

this case, since the emission-line luminosity is ~ 100 times the radio luminosity, $\varepsilon \leq 0.01$. This would in turn imply:

$$\left(\frac{V_{\rm jet}}{10^8 \text{ cm s}^{-1}}\right) \geq \left(\frac{\dot{m}_{\rm jet}}{300\ M_\odot \text{ year}^{-1}}\right)^{-1/2}.$$

From these considerations it is clear that if the emission-line region is powered by the bulk kinetic energy of the jet, then $V_{\rm jet}$ must be much larger than the observed emission-line velocities to avoid an excessive mass-loss rate from the nucleus ($V_{\rm jet} \sim 300$ km s^{-1} requires $\dot{m}_{\rm jet} \sim 3000\ M_\odot$ year^{-1}).

iii) *Formation of the Morphology*

1. *The ambient medium.*—We have presented evidence that the radio source in 3C 305 is interacting with a rapidly rotating disk-like ambient medium of unusually high density. This is probably related to the most striking aspect of the radio source, namely its relatively small size. Thus the primary interest in studying 3C 305 is to learn how a radio source is affected by the presence of such a medium. Before discussing the individual components of 3C 305, we shall consider what can be deduced about the properties of this medium.

First, information about its density comes from the value for the column density of material in the disk, $N_{\rm H} \approx 10^{22}$ cm^{-2}, which can be derived from our measured reddening and assuming a normal gas-to-dust ratio (Gorenstein 1975). Such a column density (if the gas is entirely in an atomic form) implies an H I mass interior to a radius of 2.5 kpc of $M_{\rm H\ I} \sim 1.5 \times 10^9\ M_\odot$, or $M_{\rm H\ I}/M_{\rm TOT} \sim 0.02$ (cf. § IV*b*[i]). This value is typical of early-type disk galaxies (e.g., Roberts 1975). Much of the gas might well be in molecular form, and $N_{\rm H} \sim 10^{22}$ cm^{-3} lies within the range implied by observations of molecular disks in our own and other spiral galaxies (Liszt and Burton 1978; Linke, Stark, and Frerking 1981; Bieging *et al.* 1981). $N_{\rm H} \approx 10^{22}$ cm^{-2} (two orders of magnitude greater than the corresponding value for the emission-line gas) would imply an average effective density of $n\phi = 6/t$ cm^{-3}, where t is the thickness of the gas layer in kpc.

Second, the observed emission-line velocities, if indicative of the sound speed of the ambient medium, indicate that the temperature of that medium (presumably disrupted by the advancing jet) may be $1\text{–}2 \times 10^6$ K. If the gas near the radio source is that hot, it will not be confined to a thin disk but will expand perpendicular to the disk at a velocity of several hundred kilometers per second. If we assume that the transverse extent of the region of Hα emission is indicative of the expansion of this hot gas, then $t \approx 1\text{–}2$ kpc, implying $n\phi \approx 4$ cm^{-3}.

Interestingly enough, a medium with a density $n \approx 4$ cm^{-3} and $T \approx 10^{6.2}$ K would be close to static pressure equilibrium with the radio lobes and with the optical emission-line clouds. Moreover, the luminosity in ionizing radiation from $\sim 10^9\ M_\odot$ (the approximate mass of the disrupted disk gas) with $n \approx 4$ cm^{-3} and $T \approx 10^{6.2}$ K would be $\sim 10^{44}$ ergs s^{-1}. This would be sufficient to supply the energy needed to ionize the emission-line region. The total thermal energy in such gas would be $\sim 5 \times 10^{56}$ ergs, so that the kinetic energy in the emission-line clouds and the energy in radiating relativistic particles each represent a small fraction of the total energy in the system (in agreement with the observational and theoretical ideas presented in § IV*c*(i). Moreover, the radiative lifetime ($E_{\rm TOT}/L$) of this hypothetical gas is comparable to that of the radio lobes ($10^5\text{–}10^6$ years), so both could be resupplied with energy from the jet on comparable time scales. There is thus *indirect* evidence for the existence of a diffuse medium characterized by $T \approx 1\text{–}2 \times 10^6$ K and $n \approx 1\text{–}10$ cm^{-3} and extending throughout the region of the bright radio and optical emission.

We now consider the processes by which this medium might influence the structure of the different morphological components of 3C 305.

2. *The lobes.*—Our hypothetical ambient medium could confine the lobes through static thermal pressure. On the other hand, the lobe extensions oriented roughly *perpendicular* to the radio source axis and the steep intensity gradients along the leading edge of the northern radio lobe delineate a shape that is in good accord with the original predictions of ram-pressure confinement (e.g., De Young and Axford 1967). If the lobes are advancing into our hypothetical medium ($T \approx 10^{6.2}$ K, $n = 10^{0.5}$ cm^{-3}) with a velocity $\gtrsim 300$ km s^{-1}, ram pressure should be the dominant confining mechanism.

3. *The arms.*—Another interesting morphological feature of 3C 305 is the faint radio arms that are extended nearly perpendicular to the principal radio axis. Since the arms are not rotationally symmetric, it is not attractive to explain them in terms of a wobbling ejection axis as Lonsdale and Morison (1980) have suggested.

Instead, we think it is very likely that the jets are greatly slowed or even stopped at the locations of the radio lobes. The arms may then represent plasma that escapes from the lobes and then rises buoyantly through the gaseous halo of 3C 305. Note that the high degree of polarization seen in the arms is consistent with the density of thermal material in the arms being less than the densities predicted in a gaseous halo with $n \approx 10^{-2}$ to 10^{-3} cm^{-3} according to Norman and Silk (1979). This buoyancy picture would also explain the separation of the radio and emission-line arms, since the latter are probably located within the disklike interstellar medium of 3C 305.

4. *The jets.*—Since the jets presumably have the closest connection to the energy-carrying material in 3C 305, we will consider their morphology in detail.

The jets are unresolved in the transverse direction, and hence we do not know whether they could be confined by a static thermal pressure of $\sim 3\times 10^{-9}$ dyn cm^{-2} (that of the emission-line clouds). More to the point, we do not know whether they are in fact confined at all. A free jet will expand transversely such that the cotangent of its opening angle is equal to its internal Mach number:

$$M_{\rm int} = V_{\rm jet}\left(\rho_{\rm jet}/U_{\rm jet}\right)^{1/2}.$$

If we assume (as above) that the jet kinetic energy powers the emission-line region, then

$$L_{\rm jet} = 10^{44}\ {\rm ergs\ s^{-1}} = \tfrac{1}{2}\left(\rho_{\rm jet} V_{\rm jet}^3 \sigma_{\rm jet}\right).$$

Combining these two equations, and considering the dependence of $U_{\rm jet}$ and $\sigma_{\rm jet}$ on the jet diameter (for which we have an upper limit only), we find:

$$M_{\rm int} \geq 4.1\times 10^5\ V_{\rm jet}^{-1/2}.$$

Thus, provided the jet is not relativistic (Lorentz $\gamma \sim 1$), we find (from the jet energetics alone):

$$M_{\rm int} \geq 2.3.$$

Since the radio lobes *are* resolved in the transverse direction, the ratio of lobe-width to lobe-nucleus separation (treated as the free-jet opening angle) implies $M_{\rm int} \sim 4$. Thus the radio source morphology and physical parameters derived for the jet are consistent with (but do not require) an unconfined jet.

The jet morphology shows several interesting features for which various explanations are possible. The bright *knots* in the jets could be explained in terms of intermittent ejection episodes, a pinching Kelvin-Helmholtz instability (if the jet is confined), or simply as regions in which the jet collides with a large cloud, causing particle-acceleration processes to flare up (Blandford and Königl 1979).

The series of small-scale *wiggles* evident in the jet could likewise be ascribed to Kelvin-Helmholtz instabilities (but not if the jet is free). Multiple deflections of the jet by large clouds seem unlikely, since a single inelastic collision would probably heat the jet, causing it to break-up. The most attractive possibility is that the wiggles are caused by a wobbling ejection axis (Miley 1976). Rees (1978) has suggested that such precession might occur following a galaxy merger in which the spin axes of the accreted material and nuclear "engine" are misaligned (3C 305 shows signs of a recent merger, as we shall discuss below).

An S *symmetry* is also apparent in the morphology of the bright part of the radio source. This could be a consequence of the sweeping (ram pressure) effect of the rotating disk of gas through which the jets propagate (Wilson and Ulvestad 1982; van Breugel *et al.* 1982). The transverse momentum flux provided by a disk like that in the interior of our own Galaxy would be adequate to bend a jet with properties similar to those deduced for 3C 305. However, the overall sense of bending seen in the 3C 305 jet is opposite to that expected given the orientation of the galaxy and the rotation-sense of the disk. The S shape could also be due to the buoyancy or to so-called refraction (Henriksen, Vallée, and Bridle 1981) in which the jet will appear to bend toward the projected minor axis of the galaxy (as is the case in 3C 305). Bridle, Fomalont, and Cornwell (1981) have successfully applied this model to 3C 293, a source that strongly resembles 3C 305 (van Breugel *et al.* 1982).

5. *Source deceleration and energy dissipation.*—The small overall size of 3C 305 together with the evidence for a vigorous interaction between the radio source and the ambient medium suggests that it is this interaction that brakes the source. We have seen that the existence of the radio arms can also be understood if the jets have been greatly slowed down.

We believe that the jets are braked as their kinetic energy is dissipated in an interaction with the ambient medium, an interaction which powers the emission-line gas as well as the radio source. The rotation of the gaseous disk in 3C 305 would bring $\sim 35\ M_\odot\ {\rm yr^{-1}}$ through the region where the radio jet interacts with the ambient medium (for $N_{\rm H} \approx 10^{22}$ cm^{-3} in the disk). The actual rate at which the jet and gaseous disk interact would be significantly larger than this if the jet is driving a shock wave out into the disk. Taking the spatial extent and velocity of the emission-line clouds as indicative of the shock wave would imply a rate of interaction 500 $M_\odot\ {\rm yr^{-1}}$. The dissipation of 10^{44} ergs s^{-1} into 500 $M_\odot\ {\rm yr^{-1}}$ ($\sim 3.5\times 10^{28}$ g s^{-1}) would imply that the ambient gas absorb $\sim 3\times 10^{15}$ ergs gm^{-1}, corresponding to a temperature $\lesssim 10^7$ K, or a factor 5 higher than our estimate of the temperature of the disrupted disk material. This discrepancy is not significant in light of the uncertainties in the respective estimates.

iv) *Depolarization*

Comparing the values of $n_e \phi L$ necessary to depolarize the bright part of 3C 305 at 5 GHz calculated in § III*a*(ii) above with the value of $n_e \phi L$ inferred for the optical emission-line gas in § III*c*(ii), *we see that the optical emission-line gas alone appears sufficient to depolarize the source*. Note that many assumptions have been made in deriving both the optical and radio values of $n_e \phi L$, and so several caveats must be stated.

First, it is unlikely that the ionized gas which dominates in optical line emission completely covers the bright part of the radio source, since if it did, its

emission measure ($n_e^2 \phi L$) would be sufficient to produce free-free absorption of the radio continuum at frequencies lower than ~ 60 MHz. The radio spectrum of 3C 305 (Kuhr *et al.* 1979) shows no sign of a turnover down to the lowest frequency measured (38 MHz), so the "covering factor" of the emission-line gas can be no greater than $\sim 30\%$. The emission of line radiation and the free-free opacity are both weighted by n_e^2, while the Faraday depth is weighted by n_e. Thus a more diffuse thermal medium that is associated with the emission-line gas, but has a lower density and larger covering factor, could produce the depolarization without violating the limit on free-free opacity or contributing significantly to the line emission.

Turning our attention to the geometry of such a medium, we must discriminate between a case in which the depolarizing medium is *mixed* with the radio plasma, and a case in which the depolarizing medium is *surrounding* magneto-ionic material that is inhomogeneous on a scale much smaller than the resolution in our radio map. If the depolarizing medium is intimately associated with the emission-line gas (as Fig. 5 strikingly demonstrates to be the case), the evidence favors a surrounding depolarizing medium. The strongest evidence in this sense is the location of much of the emission-line gas outside or adjacent to the regions of brightest radio emission. This is clearly seen in the vicinity of the bright Hα and radio lobes in the northeast of 3C 305, where the optical and radio features are offset by ~ 1 kpc ($\sim 1''$). This also seems to be true in all other examples of emission-line gas associated with the lobes of radio galaxies (cf. van Breugel and Heckman 1981). In such a case, the magnetic field (calculated from minimum energy considerations) *in* the radio source may or may not bear a quantitative relation to the surrounding field in which the line-emitting gas would be embedded.

Further information about whether the depolarizing material is mixed with or surrounds the radio plasma will come from radio polarization measurements at shorter wavelengths. Multifrequency depolarization calculations (e.g., van Breugel 1980) should then allow us to place more stringent constraints on the geometry of the thermal and relativistic media within 3C 305.

d) The Galaxy

Although we have gathered a large body of information about 3C 305, the most perplexing question of all remains unanswered: *Why does such an atypically small, powerful radio source occur together with such an unusually large and luminous emission-line region in such a peculiar early-type galaxy*?

One possibility is that we are witnessing the aftermath of a recent merger between a massive early-type galaxy and a late-type galaxy. In this case the powerful radio source would be produced by the early-type galaxy (possibly triggered by the "fuel" dropped into its nucleus by the gas-rich late-type galaxy). The "cannibalism" of the late-type galaxy would explain the gas, dust, and relatively young stars within the early-type galaxy, while the large one-armed spiral could be the tidal debris produced during the merger.

The rough alignment between the rotation axis of the captured gas and the minor axis of the main body of the galaxy could then be understood, if the gas has relaxed with respect to the stellar potential within the inner several kiloparsecs of the early-type galaxy. This would require that the merger took place at least several 10^8-year-long rotation periods ago.

Evidence for galaxy mergers of a similar kind has been discussed for the spindle galaxy NGC 2685 (Shane 1980), Fornax A = NGC 1316 (Schweizer 1980), and Cen A = NGC 5128 (Graham 1979), the latter two being well-known radio galaxies.

e) A Possible Scenario

As a means of tying together the various features of our discussion, we present the following possible scenario for 3C 305.

The main body of 3C 305 is a giant elliptical or S0 galaxy, and the gas, young stars, dust, etc., are the debris of a late-type galaxy which merged with 3C 305 several rotations ago. The merger triggered nuclear activity in the early-type galaxy and twin radio-emitting jets were ejected at $V \gg 10^3$ km s^{-1} (by chance) nearly into the rotating disk of gas acquired from the late-type galaxy. The supersonic passage of the jets through the disk drove shocks into the ambient gas, dissipating the kinetic energy of the jets into thermal energy. Much as in a supernova remnant, only a small fraction of the dissipated energy was transformed through shocks and turbulence into the relativistic particles and magnetic fields responsible for the observed radio emission. A comparably small fraction supplied the emission-line clouds with kinetic energy. Most of the dissipated energy was ultimately radiated away in the form of the observed emission lines (the shocks produced ionizing radiation, collisional ionization, etc.). As the kinetic energy of the jets was transformed in this way, the outward motion of the jets was braked.

The jets were thereby slowed to velocities of a few hundred kilometers per second at their termination points (the lobes) which were then confined and shaped by the ram pressure of the disk gas. Some of the decelerated radio plasma escaped and rose buoyantly out of the confining medium, leading to the formation of the radio arms.

At the confluence of the rotating quiescent disk material, the supersonically outbound jet material, and the shock-heated disk material, the situation would have been complex. Some of the gas was probably entrained in the jet and accelerated out into the galaxy disk, some of the gas was driven away from the radio source by the

blast waves created by the passage of the jet, and much of the gas retained the rotational component of its kinematics. These three types of motion were responsible for (respectively) the excitation of the Hα arms; the broad, blue asymmetric emission-line profiles; and the large-scale velocity gradient across the disk.

We emphasize that this picture is not the *only* plausible interpretation of the large body of data we have presented, but is intended to serve as a self-consistent working hypothesis.

V. CONCLUSIONS

We have presented a mountain of data concerning 3C 305, the quantitative details of which are given in the various diagrams and tables. These details should not obscure what we feel to be several key results that have emerged from our investigation. The most fascinating aspect of the data is the clear connection between the radio source and the line-emitting gas summarized at the beginning of § IV. These connections demonstrate that 3C 305 is an ideal laboratory for the investigation of the physics of extragalactic radio sources, since in it the radio plasma is vigorously interacting with a medium whose properties can be studied in great detail.

What have we learned about 3C 305 that has relevance to the study of active galaxies in general? First, several of the connections between the radio source and line-emitting gas are dependent on the assumption of minimum energy in the radio source. Unless these connections are just coincidental in 3C 305, their existence is thus indirect evidence that the energy in 3C 305 is indeed close to the minimum value. This would be an important result since the assumption of minimum energy is generally made when interpreting extragalactic radio sources despite a notable lack of evidence.

Second, the most popular model for extragalactic radio sources involves the collimated outflow from the nucleus of a fluid whose bulk kinetic energy powers the radio source. The conversion of this kinetic energy into synchrotron radiation is thought to be an inefficient process. The source 3C 305 provides quantitative evidence in support of this model since the energy loss in the form of radio synchrotron radiation is $\lesssim 1\%$ of the energy loss from the thermal material. Moreover, the connection between the larger radio luminosity and broader emission lines within 3C 305, together with the previously established statistical relation between radio luminosity and [O III] line width for kiloparsec-sized components of active galaxies is further evidence that the ambient medium plays a fundamental role in the conversion of bulk outflow kinetic energy into radio synchrotron emission. In fact, we have argued that such an interaction may ionize the emission-line gas; supply it with kinetic energy; brake, deflect, and confine the radio source; and possibly produce the radio emission itself.

Third, our discovery that the depolarizing medium in 3C 305 is intimately connected with the optical emission-line gas, most of which is located *outside* the regions of intense radio emission, may have important implications for the interpretation of depolarization in extragalactic radio sources. In particular, Faraday depolarization is generally used to argue that appreciable thermal material is mixed with the relativistic plasma responsible for the radio emission. Since this thermal material is often identified with the bulk fluid, whose kinetic energy drives the radio source, our result *may* mean that depolarization arguments overestimate the density of this energy-carrying fluid. If this is the case, then previous estimates of the jet velocities required by the radio source energetics would all be lower limits.

Finally, the possibility that the outflow velocity of the leading edges of the radio *lobes* of 3C 305 might well be comparable to the velocities observed in the optical emission-line gas (few hundred km s^{-1}) is consistent with statistical studies of component intensity ratios in double radio sources, and indicates that the expansion speeds of extragalactic radio sources may be $\lesssim 1000$ km s^{-1}. Such speeds would imply ages in excess of 10^9 years for the largest sources.

Fifth, 3C 305 shows many similarities in its radio and optical properties to Seyfert galaxies (collimated, kiloparsec-scale radio emission; morphological resemblance between the emission-line gas and radio emission; a parent galaxy with a gaseous disk; intense, broad emission lines whose kinematics are tied to the radio source). It also exhibits some important differences (very powerful radio emission, an extended region of line emission in which neither the line intensity nor line width peak at the nucleus, no evidence for a nonstellar nuclear continuum). We believe these various similarities and differences can be reconciled within the following general description of active nuclei: the nuclear engine is capable of producing a compact source of luminous energy (an ionizing nonstellar continuum) as well as a collimated outflow of a bulk fluid which produces radio emission and supplies the emission-line clouds with kinetic energy. In the case that the compact source is the dominant form of energy loss, a radio-quiet quasar or (relatively) radio-quiet Seyfert is observed. In the case that the collimated outflow is dominant, a classical radio galaxy is observed. Within the subset of active galaxies having substantial gaseous disks, the typical Seyfert and 3C 305 represent different ends of this continuum: in 3C 305 the collimated outflow supplies both kinetic and ionizing energy to the emission-line region.

Sixth, and in a related vein, 3C 305 offers at least a partial answer to the question with which we began our paper: Why is strong, extended radio emission associated with active elliptical galaxies, but not active spiral galaxies? We would argue that the presence of a substantial gaseous disk surrounding the nucleus thwarts

the outward thrust of the radio jets, and does not allow an extended (greater than galaxy sized) radio source to develop. However, the question of why *powerful* kiloparsec-sized radio cores are seldom observed in spiral galaxies remains unanswered. There is a very luminous and massive bulge component of 3C 305, and it may be that this is a prerequisite for powerful radio emission that is satisfied by few spiral galaxies.

Finally, our belief that 3C 305 represents the recent merger of a massive early-type and a gas-rich late-type galaxy contributes to the growing body of evidence linking galaxy-galaxy interactions (and galaxy mergers in particular) to nuclear activity (cf. the review by Balick and Heckman 1982*b*).

Further study of 3C 305 is called for. We have begun multifrequency observations of the radio intensity and polarization distribution with the hope of relating them in more detail to the properties of the line-emitting gas. Also, accurate measurements of the stellar kinematics will provide crucial information regarding the relation of the line-emitting gas to the ambient galaxy. Of particular importance are observations of the radio source and the optical gas with higher spatial resolution. We have seen that the physical conditions within 3C 305 resemble, in some ways, those in supernova remnants. Just as in these remnants and in some active galaxies such as NGC 1275, the gas in 3C 305 may well be distributed in filaments. Measurements with the Space Telescope can reveal whether this is the case and, if so, attempt to establish what role the filaments play in the microprocesses that result in the production of the synchrotron radio emission. In addition, theoretical modeling of the scenarios we have presented is required. This should include a hydrodynamical investigation of the time-dependent interaction in which the kinetic energy of the jet fluid is dissipated. Further work on 3C 305 holds the promise of producing important and possibly unique insights into the extragalactic radio source phenomena.

The authors are indebted to the staffs at NRAO and KPNO (particularly Garth Illingworth and Doug McElroy) for their aid in obtaining and analyzing the data on which this paper is based. We also are grateful to the Leiden/Westerbork software group for additional assistance with data analysis. G. Fabbiano, R. Kirshner, C. Lonsdale, and A. Wilson are thanked for useful conversations and for access to unpublished data that were important in interpreting our data. The comments and advance of R. Mushotsky, J. Dickel, M. Begelman, R. Blandford, and D. De Young were also valuable. We want to especially thank Betty Schueler for her usual excellent job in typing and editing this manuscript. T. M. H. thanks the President's Club of the University of Arizona for financial support in the form of a Bart Bok Fellowship (during the tenure of which this work was concluded) and Sterrewacht Leiden for travel support during the early observational stages of this work. B. B. gratefully acknowledges grants from the Graduate Student Research Fund of the University of Washington and from the Research Corporation. The work was partially supported by NATO grant 1828.

REFERENCES

Baldwin, J. A., Phillips, M. M., and Terlevich, R. 1981, preprint.
Balick, B., and Heckman, T. 1979, *A.J.*, **84**, 302.
_____. 1982*a*, in preparation.
_____. 1982*b*, *Ann. Rev. Astr. Ap.*, **20**, in press.
Bieging, J. H., Blitz, L., Lada, C. J., and Stark, A. A. 1981, *Ap. J.*, **247**, 443.
Blandford, R. D., and Königl, A. 1979, *Ap. Letters*, **20**, 15.
Bridle, A. H., Fomalont, E. B., and Cornwell, T. J. 1981, preprint.
Brown, R. L., and Gould, R. J. 1970, *Phys. Rev. D.*, **1**, 2252.
Butcher, H. R., van Breugel, W., and Miley, G. K. 1980, *Ap. J.*, **235**, 749.
Chevalier, R. A. 1977, *Ann. Rev. Astr. Ap.*, **15**, 175.
Cowie, L. L., Fabian, A. C., and Nulsen, P. E. J. 1980, *M.N.R.A.S.*, **191**, 399.
De Young, D. S., and Axford, W. I. 1967, *Nature*, **216**, 129.
Fabbiano, G. 1981, private communication.
Faber, S. M., and Gallagher, J. S. 1976, *Ap. J.*, **204**, 365.
_____. 1979, *Ann. Rev. Astr. Ap.*, **17**, 135.
Fosbury, R. A. E., Mebold, U., Goss, W. M., and Dopita, M. A. 1978, *M.N.R.A.S.*, **183**, 549.
Gorenstein, P. 1975, *Ap. J.*, **198**, 95.
Graham, J. A. 1979, *Ap. J.*, **232**, 60.
Graham, J. A., and Price, R. M. 1981, *Ap. J.*, **247**, 813.
Heckman, T. M. 1980*a*, *Astr. Ap.*, **87**, 142.
_____. 1980*b*, *Astr. Ap.*, **87**, 152.
Heckman, T. M., Balick, B., and Crane, P. C. 1980, *Astr. Ap. Suppl.*, **40**, 295.
Heckman, T. M., Illingworth, G. D., Miley, G. K., and van Breugel, W. J. M. 1982, in preparation.
Heckman, T. M., Miley, G. K., van Breugel, W. J. M., and Butcher, H. R. 1981, *Ap. J.*, **247**, 403.
Henriksen, R. N., Vallée, J. P., and Bridle, A. H. 1981, *Ap. J.*, **249**, 40.
Hoessel, J. G., Gunn, J. E., and Thuan, T. X. 1980, *Ap. J.*, **241**, 486.
Högbom, J. A. 1974, *Astr. Ap. Suppl.*, **15**, 417.
Kirshner, R. P. 1974, *Ap. J.*, **194**, 323.
_____. 1981, private communication.
Koski, A. T. 1978, *Ap. J.*, **223**, 56.
Kuhr, H., Nauber, U. Pauliny-Toth, I. I. K., and Witzel, A. 1979, Max-Planck-Institute für Radioastronomie preprint 55.
Linke, R. A., Stark, A. A., and Frerking, M. A. 1981, *Ap. J.*, **243**, 147.
Liszt, H. S., and Burton, W. B. 1978, *Ap. J.*, **226**, 790.
Lonsdale, C. J., and Morison, I. 1980, *Nature*, **288**, 66.
Lonsdale, C. J., *et al.* 1981, private communication.
McKee, C. F., and Hollenbach, D. J. 1980, *Ann. Rev. Astr. Ap.*, **18**, 219.
Miley, G. K. 1976, in *Proc. NATO Summer School, "Physics of Nonthermal Radio Sources,"* ed. G. Setti (Dordrecht: Reidel).
_____. 1980, *Ann. Rev. Astr. Ap.*, **18**, 165.
Miley, G. K., Heckman, T. M., Butcher, H. R., and van Breugel, W. J. M. 1981, *Ap. J. (Letters)*, **247**, L5.
Miley, G. K., van Breugel, W. J. M., Heckman, T. M., Butcher, H. R., and Balick, B. 1982, in preparation.
Netzer, H. 1981, preprint.
Norman, C., and Silk, J. 1979, *Ap. J. (Letters)*, **233**, L1.
Nussbaumer, H., and Osterbrock, D. E. 1970, *Ap. J.*, **161**, 811.
Osterbrock, D. E. 1974, *Astrophysics of Gaseous Nebulae* (San Francisco: Freeman).
_____. 1977, *Ap. J.*, **215**, 733.
_____. 1981, *Ap. J.*, **246**, 496.
Owen, F. N., Hardee, P. E., and Bignell, R. C. 1980, *Ap. J. (Letters)*, **239**, L11.
Pelat, D., Alloin, D., and Fosbury, R. A. E. 1981, preprint.
Raymond, J. C., and Smith, B. W. 1977, *Ap. J. Suppl.*, **35**, 419.

Rees, M. J. 1978, *Nature*, **275**, 516.
Rees, M. J., Begelman, M., and Blandford, R. D. 1981, preprint.
Roberts, M. S. 1975, in *Galaxies and the Universe*, ed. A. Sandage, M. Sandage, and J. Kristian (Chicago: University of Chicago Press), p. 309.
Robinson, W., Ball, W., Vokac, P., Piegorsch, W., and Reed, R. 1979, in *Proc. SPIE, Instrumentation in Astronomy III*, **172**, 98.
Rubin, V. C., Ford, W. K., Jr., and Thonnard, N. 1978, *Ap. J. (Letters)*, **225**, L107.
Sandage, A. 1966, *Ap. J.*, **145**, 1.
Schechter, P. L., and Gunn, J. E. 1979, *Ap. J.*, **229**, 472.
Schwarz, U. J. 1978, *Astr. Ap.*, **65**, 345.
Schweizer, F. 1980, *Ap. J.*, **237**, 303.
Shane, W. W. 1980, *Astr. Ap.*, **82**, 314.
Shuder, J. M. 1982, *Ap. J.*, **259**, in press.
Thompson, A. R., Clark, B. G., Wade, C. M., and Napier, P. J. 1980, *Ap. J.*, **240**, 974.
Turnrose, B. E. 1976, *Ap. J.*, **210**, 33.
Ulrich, M.-H., and Péquignot, D. 1980, *Ap. J.*, **238**, 45.
van Breugel, W. J. M. 1980, *Astr. Ap.*, **81**, 265.
van Breugel, W. J. M., and Heckman, T. M. 1981, in *IAU Symposium 97, Extragalactic Radio Sources*, ed. D. S. Heeschen and C. M. Wade (Dordrecht: Reidel), in press.
van Breugel, W. J. M., Heckman, T. M., Butcher, H. R., and Miley, G. K. 1982, in preparation.
van der Kruit, P. C., Oort, J. H., and Mathewson, D. S. 1972, *Astr. Ap.*, **21**, 169.
Wilson, A. S., and Ulvestad, J. S. 1982, preprint.
Wilson, A. S., and Willis, A. G. 1980, *Ap. J.*, **240**, 429.
Yee, H. K. C. 1980, *Ap. J.*, **241**, 894.
Yee, H. K. C., and Oke, J. B. 1978, *Ap. J.*, **226**, 753.

B. BALICK: Department of Astronomy, University of Washington, Seattle, WA 98195

H. R. BUTCHER and W. J. M. VAN BREUGEL: Kitt Peak National Observatory, P.O. Box 26732, Tucson, AZ 85726

T. M. HECKMAN: Astronomy Program, University of Maryland, College Park, MD 20742

G. K. MILEY: Sterrewacht Leiden, Postbus 9513, 2300 RA Leiden, The Netherlands